UNIVERSITY OF OKLAHOMA

GRADUATE COLLEGE

ON THE RELATION BETWEEN ENVIRONMENTAL WIND VEER AND CIRCULATION IN SEVERE STORMS

A DISSERTATION

SUBMITTED TO THE GRADUATE FACULTY

in partial fulfillment of the requirements for the

degree of

DOCTOR OF PHILOSOPHY

BY

JOSEPH L. GOLDMAN

Norman, Oklahoma

1971

ON THE RELATION BETWEEN ENVIRONMENTAL WIND VEER

AND CIRCULATION IN SEVERE STORMS

APPROVED BY

Eugene M. Wilkins

Arthur Bernhart

DISSERTATION COMMITTEE

ABSTRACT

ON THE RELATION BETWEEN ENVIRONMENTAL WIND VEER AND CIRCULATION IN SEVERE STORMS

It has been observed that circulation is related to the environment of severe storms. Forecasting techniques use vertical variation of the environment as a forecasting parameter. A simplified model of the growing storm is used to describe atmospheric conditions which are evaluated to find characteristic ratios for use in the analysis. The early morphology of the severe storm is considered quantitatively, wherein a balance occurs between the converged low level momentum and the obstructed momentum of the middle level air flow.

Mathematical formulations are derived for the storm's motion and individual functions are presented to represent various individual physical factors that may contribute to the motion. Detailed consideration is given to two of these factors, while the remaining factors are described for future use.

The effect of environmental wind veer with height on the motion of the storm is considered through analogy with a hydrodynamic experiment of curving motion of an immersed cylinder. Qualitative agreement with the theory is shown in an experiment in which a cylinder is moved in a

curved path through a stationary fluid. The force that provides rotation about the swivel is analogous to the ambient air that changes direction with height and forces the storm to move in a curved path. For paths curved anticyclonically the vorticity imparted to the storm is cyclonic. Calculations of atmospheric circulation induced in this manner are shown to be significant and comparable to tornadic circulation.

Comparison of the theoretically computed streak lengths with the experimentally measured values shows that circulation of the correct sign is present in the fluid; however, a non-uniform distribution of ill-defined streaks due to a combination of experimental difficulties precluded exact quantitative verification. Development of better fluid tracers as well as better photography techniques will provide further verification of the analogy.

The eddy viscosity influences the drag on the storm which causes the storm to curve during its growth. The increased mixing at the periphery of the storm between ambient air and storm air increases the storm's response to momentum at higher altitudes, which results in its curved path. If the hydrodynamic analogy between the curving cylinder experiment and the curving storm path is valid, then the curved path due to a veering environment causes cyclonic circulation to exist about the storm of a magnitude comparable to twice the vorticity of the curving path. The vorticity induced at the periphery of the storm is the vorticity due to the curvature of the path, and the source of this vorticity is the

environmental winds that veer with height.

ACKNOWLEDGEMENT

The author wishes to thank all those persons who have cooperated with this study.

My deepest appreciation is expressed to Professor E. M. Wilkins for his guidance, support and encouragement on all aspects of the study, especially the theoretical and experimental; to Dr. E. W. Friday for his assistance on the design and construction of experimental equipment; to Professor Y. Sasaki for his continued encouragement, guidance and criticism of the theoretical work; to Professor W. J. Saucier for his continued support and encouragement; and to other University of Oklahoma faculty, including my graduate committee.

To my colleagues with whom much of this work has been discussed, including the staff members of the Institute for Storm Research who have provided the necessary support for my activities, and to Misses Jayne Jones and Gloria Guidry for their support during the preparation of this manuscript, I extend my gratitude and appreciation.

I am honored to extend my warmest feeling of gratitude to my colleague, Dr. John C. Freeman, and to my family, without whose encouragement and sacrifice this work could not have been accomplished. I hope their patience and understanding will have been well invested.

The equipment and technical support for experimental work was sponsored by ESSA Satellite Laboratory under Grant E-41-67-(G). All of the

experimental equipment was built at the Oklahoma University Research Laboratory, and all experiments were carried out at the mesometeorological laboratory of the Department of Meteorology. Data from the National Severe Storms Laboratory of ESSA (NOAA) was analyzed during this study. I am grateful for the use of these facilities.

TABLE OF CONTENTS

LIST OF TABLES

LIST OF ILLUSTRATIONS

ON THE RELATION BETWEEN ENVIRONMENTAL WIND VEER AND CIRCULATION IN SEVERE STORMS

I - INTRODUCTION

A. General Discussion of Storm Growth

The environment in which severe storms develop is characterized by complexity of the atmosphere. It is divided into layers of differing wind velocities and moisture distribution varying with height. The variation of moisture is related to the veering (turning clockwise) and shearing (increasing in speed) of the lower atmosphere, with the largest variation found in the two lower layers of converging air. The moisture distribution varies abruptly from moist to dry through a temperature inversion that caps the moist air in the lower levels.

Although each case of severe storm environment will undoubtedly have differing environmental temperature and moisture, the general characteristics of wind and moisture distribution appear in models useful for forecasting. To make the severe storm amenable for study, a model of the storm in an environment containing only the essentials is described. In this simplified environment the wind is assumed to be increasing in speed with height (shearing) and changing direction in a clockwise sense

with height (veering). The moisture distribution has a discontinuity, an inversion layer, where warm and very dry air caps the moist air below. Through the inversion the wind direction changes abruptly from southerly to westerly (usually SSE to SSW). The top of the environmental atmosphere governed by the stability associated with the stratosphere, decelerates the upward motion of the storm air and limits its extension into the stratosphere. This environment resembles the Great Plains condition in the spring, the place and time when most severe storms occur.

As the cloud grows in the simplified environment, southerly momentum from low levels is continuously transported upward within the cloud. An accompanying downdraft may transport westerly momentum downward simultaneously. As the cloud extends to higher altitudes the westerly momentum mixes with the southerly momentum in the cloud to give a resultant motion vector in the west of south direction. As the cloud grows deeper into the westerly current, the westward component increases, giving the storm a path curved anticyclonically.

Initial movement will be from the south in the same direction as the air below the cloud base. As the cloud grows upward (increasing in height) and outward (increasing in diameter) it becomes more influenced by the upper level air. The change in motion serves to increase the relative inflow, which increases convergence of the low level air. If conditions are sufficient for continued growth and movement in a curved path, circulation may be imparted so that the storm's direction of motion

differs from the direction of any ambient wind within its depth.

During this stage of development, when the storm's motion is different from the wind in any layer within the depth of its environment, the storm is in a quasi-steady state and has the following characteristics:

(a) It contains a single, giant circulation cell which is its simplest structure.

(b) It usually lasts for a number of hours.

(c) Intense rainshowers, giant hailstones, and tornadoes are frequently observed.

Although the mechanics of the breakup of a severe storm are not well known, general agreement exists that there is a decrease in the upward flux of moist air which allows the top of the storm to be carried away (blown off) by high-speed westerly winds. The most obvious cause of a decrease in upward flux of moist air is a decrease in available potential instability in the lower levels where air is converged into the storm, and a decrease in moisture, or temperature of converged air which may be sufficient to eliminate the necessary production of latent heat by condensation that supports the updraft.

B. The Scope of this Study

This study will treat the storm from the time it becomes influenced by the air above its cloud base to the time vorticity is imparted to it.

Examples of storm growth and motion will be given as well as an attempted explanation as to why some storms move in a curved path.

The effect shown through experimental analogy is how the curved motion of the storm cloud manifests a circulation in the environment about the storm.

II - DEVELOPMENT OF THE STORM MODEL

A. Description of the Cylindrical Storm Model

In nature, the storm is probably composed of one major and one or more minor vertical circulation cells. It is simplified in this study to one vertical circulation cell throughout its depth with minor vertical circulations at the base and top. This simplified model is supported by much descriptive work, Goldman (1962), Fujita (1963), and Browning (1964), which shows that the most severe storms contain the smallest number of cells. The minor circulation cells at the bottom are the cumulus and small towering cumulus that surround the major vertical motion and are usually connected at the base. This gives the storm the appearance of having a larger diameter at its base than at the top. These minor circulations also raise the inversion around the major storm updraft.

The circulations at the top are due to the air spreading as it is kept from penetrating far into the stratosphere. These circulations are visible at the edge of the "anvil top" on the upwind side where the abundance of dry ambient air helps to delineate the boundary of the cloud by evaporation. The wind enhances the vertical circulation by its high speed relative to the speed of cloud elements (causing overturning at the edge of the cloud mass). If there were no ambient airflow, circulation

at the top would be similar to the hydrodynamic analogy of a jet impinging on a horizontal wall as sketched in Figure 2.1. The overturning that mixes the velocities is not included as part of the model even though the result (a mixed profile) is included.

A detailed model of the ambient flow consisting of five layers of differing motion characteristics and two adjacent layers of differing moisture has been developed to represent the severe storm. (See Goldman, 1968) This model is consistent with the storms that occur in the Great Plains area, the geographic location of the maximum frequency of severe storms. In this model, the inflow layers consist of a layer of moist air covered by a layer of dry air that combines to develop the rain cooled air, cold air outflow. Since our principal concern is with the storm's motion, the depiction of the storm will be simplified by neglecting the dry air inflow layer that provides the cold air. A further simplification will be made by ascribing a cylindrical shape with values to the otherwise general model.

The depth of the storm (from base to top) is 15 km.* Its lower, middle, and upper diameters are 30 km, 10 km, and 80 km, respectively. The general shape of the storm is cylindrical in the middle layers with the top and bottom resembling the ends of a spool with a plume streaming out of

* For simplicity the storm dimensions are chosen to be to the nearest 5 km of that which is usually observed visually, photographed, or measured by the various weather radars.

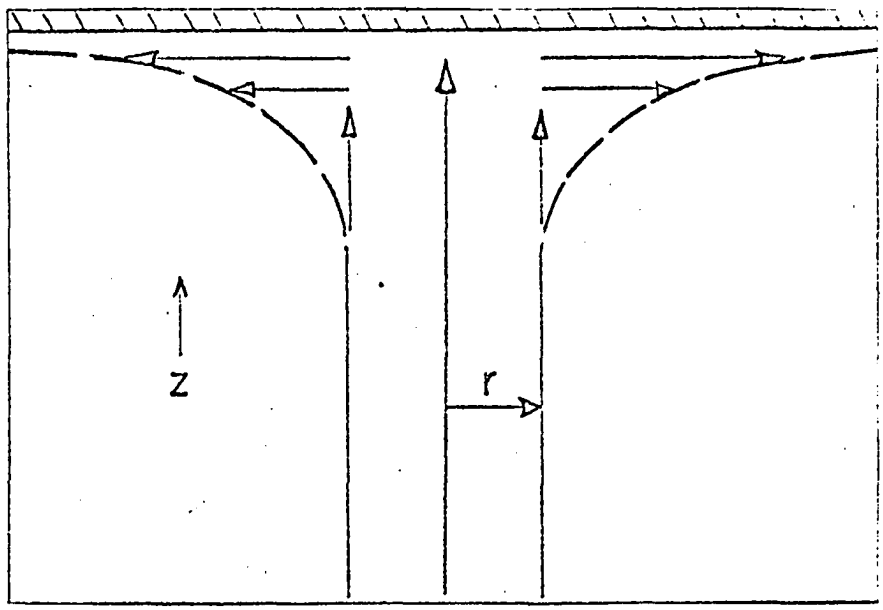

Figure 2.1 Sketch of a jet impinging on a wall. This is analogous to the flow near the storm top, in the anvil, for a negligible horizontal ambient wind velocity.

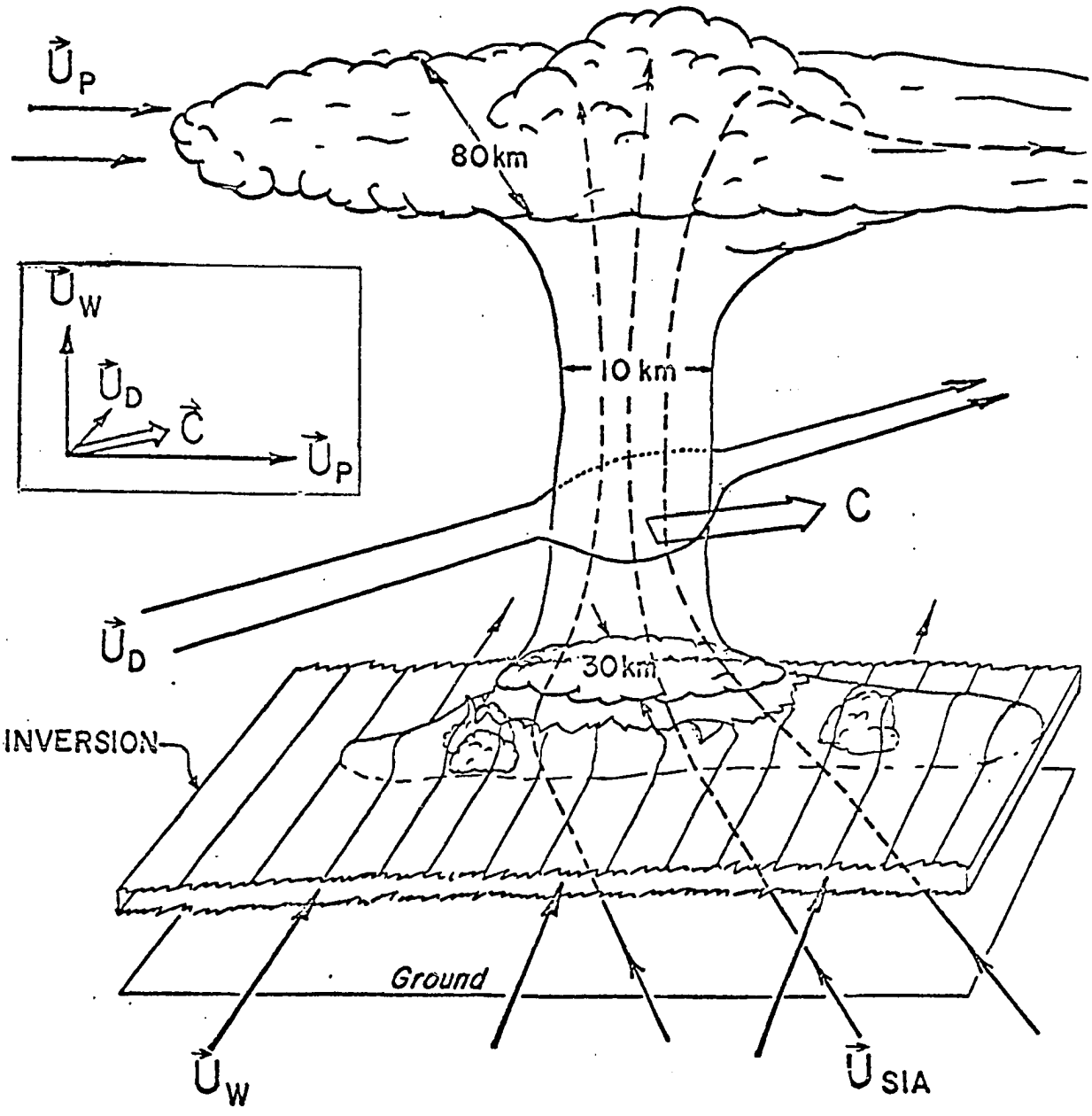

Figure 2.2 Perspective view of the simplified storm model. Inversion is broken through at the storm. See text for definition of symbols.

the top. The shape of the top is somewhat elliptical in front with the major axis oriented parallel to the ambient wind direction (and a streamer out the back). The term "anvil top" best described the side view of the storm top. The location of the cylindrical shape extending down to the low levels is approximately at the upwind focus of the elliptical-shaped top. Figure 2.2 is a perspective view of the simplified storm, and Figure 2.3 is the top view. A few large storms viewed from aircraft verify this description.

With this simple generalized form of the storm cloud established, we can add a few details that will be useful in evaluating terms in the equations of motion of the storm. The lower portion (30 km) and the upper portion (80 km) are considered hydrodynamically rough because of their obvious eddy activity, while the middle portion is considered to be relatively smooth.

B. Consideration of Environmental Flow Around Storm

Flow around a barrier is developed (as in most hydrodynamics) as a pure flow of fluids as if no barrier existed. In fixed coordinates the instantaneous stream-lines for a moving cylinder are the same as those for a doublet (source-sink combination). The doublet as shown in Figure 2.4 has a velocity vector $\vec{v}$ everywhere on a certain circle and the flow inside that circle can be replaced by a solid cylinder (or barrier) moving at speed $\vec{v}$. (The same flow results outside the circle with either the doublet or the cylinder).

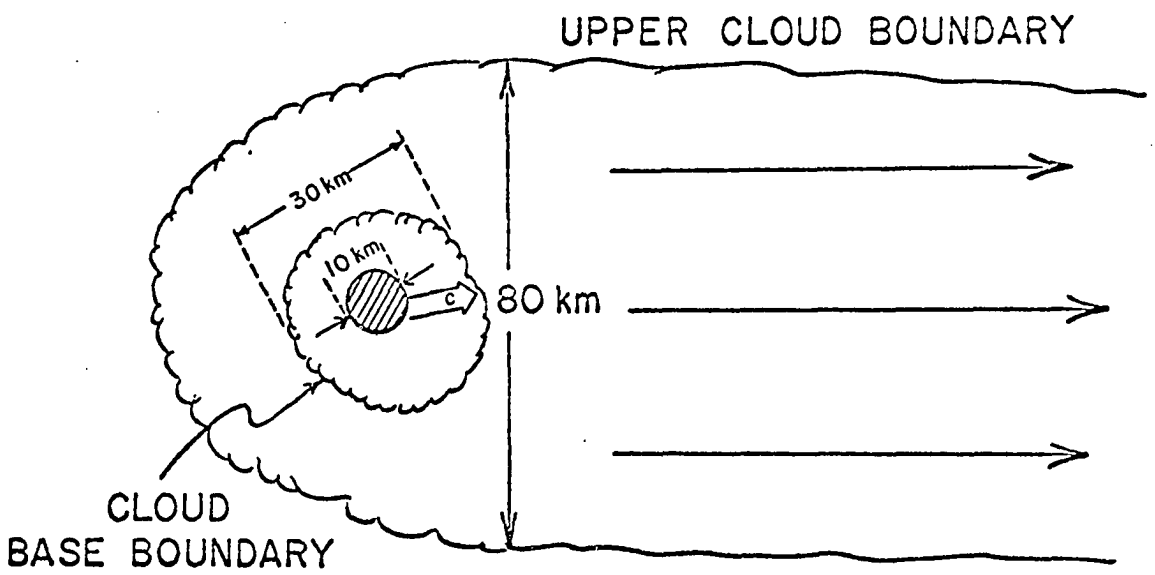

Figure 2.3 Top view of the storm.

The doublet flow may be unfamiliar because the flow around a cylinder is usually studied relative to the cylinder (or in relative coordinates). If a velocity vector $\vec{v}$ is subtracted from the doublet flow everywhere, the flow in Figure 2.5 results. In the relative coordinates moving with the cylinder the doublet is confined to the inside of the circle and the flow around the circle is the familiar flow around a cylinder or air foil. This flow can be created by just streaming fluid past a doublet, but it is more common to create the flow outside the cylinder by moving a cylinder in a fluid (in a tow tank) or streaming fluid past the cylinder (in a wind tunnel). In either case the flow seen from the cylinder is the relative flow in Figure 2.5. If the cylinder is moving, then the flow in fixed (non-relative) coordinates is as in Figure 2.4.

In this study most of the motion will be discussed relative to a moving "cylinder", the giant thunderstorm cloud.

Logic dictates that an isolated severe storm be treated as a barrier with ambient air flowing around it. This logic can best be accepted by considering a simple analogy. Suppose we have a long trough of kerosene and we allow colored water from a hose to flow into it. The flow rate of the water is sufficient to assure a continuous stream. Now move the hose from one end of the trough to the other. Since the kerosene is displaced by the "cylinder" of water from one end of the trough to the other, there must be hydrodynamic barrier flow of kerosene around the water, i.e.,

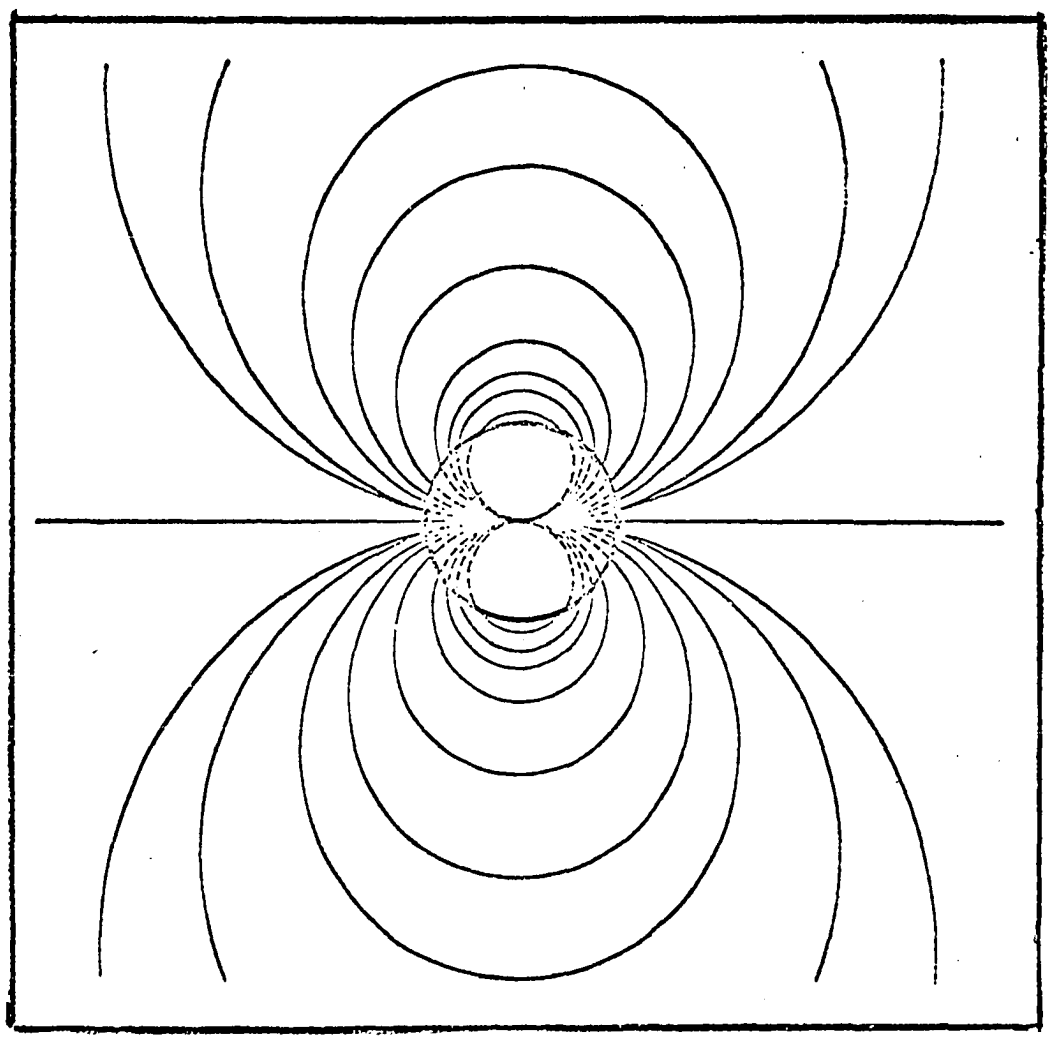

Figure 2.4 Flow around a cylinder with velocity $\vec{v}$ seen in fixed coordinates.

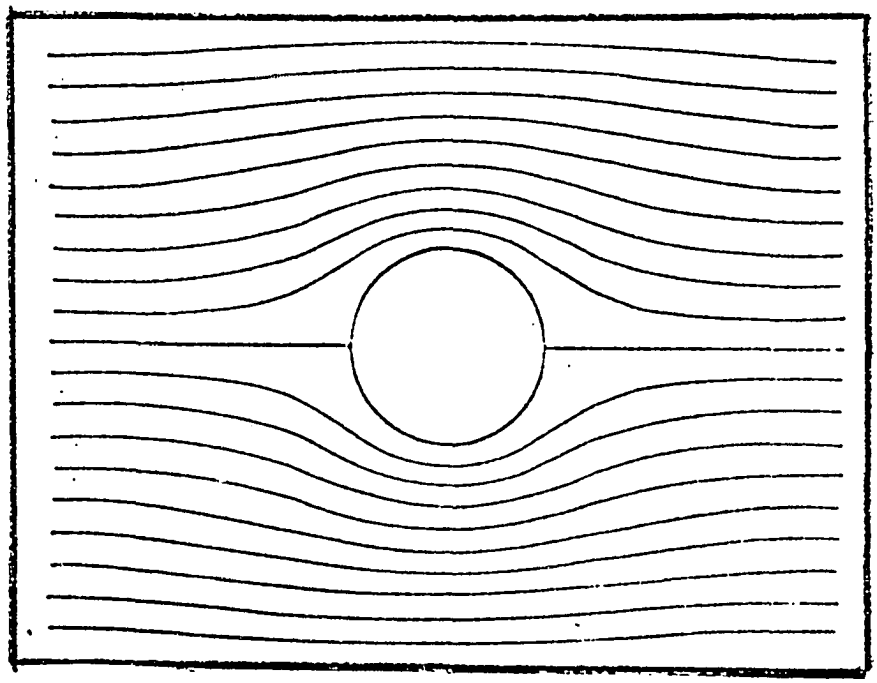

Figure 2.5 When a velocity $\vec{v}$ is subtracted from the flow, to put it into relative coordinates, the traditional picture of flow around a cylinder results. The doublet flow is now inside the cylinder.

the hose could be extended through the kerosene and almost the same flow would result.

In a very real sense a large, strong updraft, severe thunderstorm imitates the water-kerosene flow. The moist air rises until it is warm and becomes a jet of upward flowing moist air through dry air. This moist air rises to the tropopause and spreads out. The moist jet moves relative to the middle level dry air and must serve as a hydrodynamic barrier.

C. The Description of the Storm's Motion

As is shown in Figure 2.2, the storm velocity, $\vec{C}$, is directed between the upper and lower velocities. We define all of the air velocity relative to the storm by

$$\vec{U} = \vec{V} - \vec{C} \qquad (2.1)$$

where $\vec{V}$ is the velocity relative to the ground. All motion is formulated to be relative to the storm. A stationary object would have a relative velocity $-\vec{C}$ relative to the storm. A wind normal to the vector $\vec{C}$ would have a $-\vec{C}$ added to it and the resultant would be directed toward the storm of the front side. The use of relative coordinates allows motion to be correlated with obvious features of the storm such as the cloud plume (top view of storm).

Using the subscripts P, D, W for the upper (plume level -- the level of the anvil top where the plume occurs), middle (dry level), and low (wet level) respectively, we can draw a hodograph of the undisturbed environmental flow relative to the storm. This is shown in the inset of Figure 2.2 with the relative streamlines drawn on the perspective view of the storm.

We now discuss the antecedents of the air affecting the cloud motion. A considerable amount of vertical shear exists between the air-flow just below the inversion and the sub-inversion air near the ground. The air affecting the cloud's motion by momentum mixing at the cloud's edge is in the cloud (occurring from the cloud base to the inversion level), and the air that affects the motion by conserving its momentum is below the cloud. If we define $\vec{U}_{sia}$ (velocity of the sub-inversion air) as the velocity of that air that will be drawn into the storm, and $\vec{U}_W$ as the velocity of that air in and just below the inversion and in the cloud, then most of the air that mixes with storm air at the cloud boundary as it rises has ambient velocity, $\vec{U}_W$.

In this simple model the relative speeds of lower, middle and upper winds are 10, 3, and 30 m sec^{-1} respectively.

D. Formulation of the Forces

The existence of the storm in the complex multi-layered environment causes momentum exchange through inflow layers and forces in the other layers that control the storm's motion. In order to solve the motion problem, we formulate the acceleration of the storm as being the result of a combination of all the forces that could act and are significant in the storm's motion. Both descriptive and analytical symbols are used to represent the forces. The acceleration of the storm is given by

$$\frac{d\vec{C}}{dt} = \frac{1}{m}\frac{d(M\vec{U}_{sia})}{dt} + \frac{1}{m}\int_{W}^{P} \vec{F}/h\, dz + \frac{1}{m}\int_{W}^{P} \vec{F}_{K-J} dz$$

$$+ \vec{R}_{PR} + \frac{1}{\rho}\vec{\nabla}P \text{ diff.} \qquad (2.2)$$

where $\vec{C}$ is the storm's velocity and its time rate of change, $\frac{d\vec{C}}{dt}$, is the acceleration. The terms on the right side of the equation, multiplied by $\frac{1}{m}$ explicitly (for the first three) and implicitly (for the last two), represent the time rate of change of momentum of the storm, the drag force, the lift force, the propagation effects, and the pressure differential, (m is the mass of the storm) respectively. Each of the five terms is defined below, separately.

The first two terms are treated in detail while the other terms are discussed and given a suggested formulation for future use.

1. Change of Momentum Term

Since the storm is fueled from the conversion of water vapor to liquid in the rising converged sub-inversion air, the imparting of this air's momentum to the storm would have some effect on the entire storm's motion. If $\vec{U}_{sia}$ represents the velocity of the sub-inversion air that is converged into the storm, then there is a contribution to the acceleration of the storm due to the loss in horizontal momentum of this air which can be represented by $\mathcal{S}\vec{U}_{sia}$ where $\mathcal{S}$ is the mass of air taken into the storm per unit time. Note that $\vec{U}_{sia}$ is velocity relative to the storm. Since $\vec{U}_{sia}$ is a function of both the ambient flow relative to the ground and the storm motion, then it changes with either the low level environmental air motion or the source strength.

This momentum is transferred to the storm because the air has no horizontal velocity relative to the storm as it moves upward within the moving column of updraft toward the tropopause, near the storm top. In the absence of compensating forces the storm would accelerate in the direction of this relative velocity.

It will be shown that the storm can move at a constant velocity under certain conditions, but in order to do this we formulate the acceleration and show it is zero. Thus

$$\rho \frac{\pi}{4} D^2 h \vec{A}_s = \vec{U}_{sia} \not{S} \qquad (2.3)^*$$

would be true and we would have an acceleration if there were no other "forces" acting on the storm. $\vec{A}_s$ is the storm acceleration, D and h are the diameter and height of the cylinder representing the storm volume, and ρ is the air density.

2. Drag Force

The effect of the drag of the ambient air on the storm is the integrated effect throughout the depth of the storm cloud. The entire effect of drag is represented by the integral of the force, F, per depth, h, of the cloud over the entire depth from the cloud base level, W, to the top level, P. The force per unit depth is given by

$$\frac{\vec{F}}{h} = \frac{1}{2} \rho \vec{U}^2 D C_D \qquad (2.4)$$

where ρ is the density (considered to be different constants in each of the three layers), $\vec{U}$ is the ambient velocity relative to the storm at that particular level and C_D is the drag coefficient which is expected to be related

* The term $\vec{U} \frac{d}{dt} D^2$ drops out because we only consider $\vec{U} = 0$, which is the value at the initial time.

to the particular eddy viscosity at that level.

3. Lift Force

The third term is the integral of the transverse force that arises due to circulation about the storm. This force is due to the Kutta-Joukowski law that is the principle behind the lift force in aerodynamics. The transverse force (per unit length) is given by

$$\vec{F}_{K-J} = -\rho\Gamma\vec{U} \tag{2.5}$$

where ρ is the air density, $\vec{U}$ is the relative velocity, and Γ is the circulation about the storm.

Just as the drag force was integrated throughout the storm's depth, the lift force is also integrated throughout the three differing layers, taking the varying density and relative velocity into account. The varying circulation about the storm in each of the three layers is also taken into account. Depending on the method by which circulation is induced in the ambient air, the distribution of circulation with height can vary from large positive in the W layer to large negative in the P layer. Some of the processes by which circulation can be induced in the ambient air are: (1) conservation of angular momentum as the air is converged in the lower layers, (see Goldman, 1966), (2) diffusion of vorticity outward from a central updraft in solid rotation (Browning and Fujita, 1965), and (3) circulation (in the form of shear flow or "curving flow") in the ambient air upstream from

the storm (Goldman, 1966, Darkow, 1969).

4. Propagation Effects

The fourth term is the acceleration due to propagation effects. These effects are caused by generation toward the region of maximum thermodynamic instability (including moisture source) and decay in the opposite direction. This is seen most commonly in eastward moving squall lines where the generation occurs on the southern end and decay on the northern end. Newton and Fankhouser (1964) have described this motion toward the source of moisture and have formulated a function that is based on the knowledge of the moisture source. For our purposes the function should be related to the dynamic mechanism that forces the storm to move in that direction. Although this function is yet to be formulated, some necessary requirements may be listed.

The term for propagation effects is called a residual acceleration, $\vec{R}_{PR}$. We expect that the term is made up of a number of factors that contribute to convection such as moisture, stability, low-level convergence and even surface roughness. These terms can be written as $K \vec{\nabla} Q$ where Q is the quantity that contributes to convection.

Empirical evidence derived from forecast verifications has shown us that the axis of maximum instability, the axis of maximum low level and high level wind flow (the so-called "low level jet" and the "jet stream"), and the middle level axis of maximum moisture are important for locating

the initiation of severe storms (Miller, 1967). The geographic location of the intersection of these axes makes up the location of the forecast center of convective activity. Just as the initiation of convection has been shown to be related to these axes, the propagation (or in rebirth of convection) is expected to be related to gradients associated with the axes of these quantities. The residual term may be formulated as:

$$R_{PR} = K_1 \vec{\nabla} s + K_2 \vec{\nabla} M + K_3 \vec{\nabla} U_P + K_4 \vec{\nabla} U_{sia} \qquad (2.6)$$

where s is the stability index, M is the middle level moisture and U_P and U_{sia} represent the jet stream velocity and the converged part of the low level jet respectively. The coefficients K_1 through K_4 are determined empirically and are not restricted to be constants.

5. Pressure Differential

Because of the veering environment in which most severe storms are embedded, the distribution of hydrostatic pressure about the storm is not symmetrical. In an environment such as the Great Plains where the relative wind from the south at cloud base veers to the west at the top, the pressure measured at the ground, due to the integrated pressure throughout the storm's depth, is lower on the forward side of the storm.

The principal contributor to this asymmetric pressure distribution at the ground may be the low pressure associated with the smaller air

density in the anvil cloud (see Figure 2.6). This would then cause an acceleration of the storm in the direction of the low pressure. The magnitude of the acceleration would be dependent on the thickness of the anvil cloud, and to a lesser extent, the vertical acceleration of the air in the clouds. A description of the pressure distribution of this type, but on a larger scale, is given by Bonner (1962). The pressure would be lowest beneath the anvil cloud extending in the direction of the upper winds.

The momentum conservation term and the drag force term in combination can provide an infinite number of constant velocities for the storm embedded in an environment in which the wind changes direction and speed with height. As seen above, the drag is an important contributing factor to the resulting velocity. When applying the classically developed relationships of drag on a cylindrical body, we are restricted to the empirical evidence that treats the atmosphere as a turbulent medium represented by supercritical Reynolds numbers. However, we are considering that the updraft of the storm system manifest by the visual cloud acts like a cylindrical barrier to the horizontal motion of the ambient air.

E. Consideration of the Balance of Drag and Momentum Change

During the initial development of the storm, when the cloud is

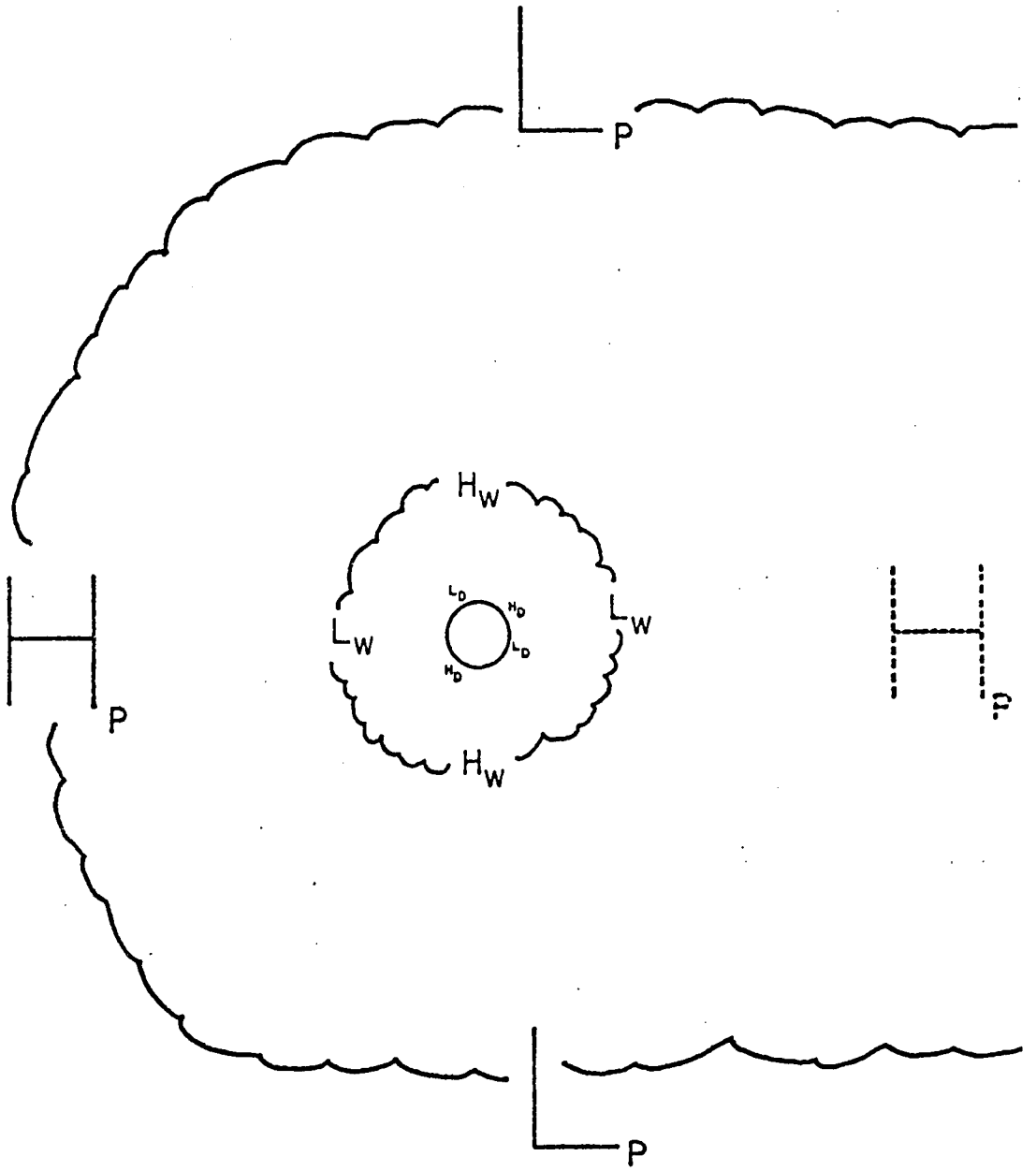

Figure 2.6. Schematic of the Bernoulli pressure at three levels of the storm for the top view of Figure 2.3. The size of the highs (H) and lows (L) at the various levels indicate comparable magnitude. The dashed high at the P level represents the consideration that air density of cloud may contribute to low pressure there.

forming, the first term in the acceleration equation is probably the most significant. As the storm continues growing upward into the middle layer where the ambient air flow varies significantly from the lower layer, the significance of the second term, the drag force, increases. During this time the pre-storm cloud (in its early stage of development) moves under the influence of these terms. We therefore consider how these terms may balance each other and the consequences of this balance.

The time rate of change of momentum is given as in equation (2.3) and the drag force is rewritten as

$$\vec{F} = \frac{\rho}{2} C_D \ \vec{U}_M \left| \vec{U}_M \right| hD \qquad (2.7)$$

where $\vec{U}_M$ is the relative velocity of the middle layer air.

The storm column is moving at speed $\vec{\mathcal{C}}$ which is considered in relative coordinates, with, $\vec{U}_{sia}$, the relative velocity of lower moist air and, $\vec{U}_M$, the average relative velocity of middle layer air, moving at constant speed ($\vec{A}_s = 0$).

$$\rho \frac{\pi}{4} D^2 h \vec{A}_s = \vec{U}_{sia} \mathcal{G} + \frac{\rho}{2} C_D \ \vec{U}_M \left| \vec{U}_M \right| hD \qquad (2.8)$$

If we set $\vec{A}_s = 0$, then one obvious condition for a steady state (a storm moving at constant speed) is that the vectors $\vec{U}_{sia}$ and $\vec{U}_M$ oppose each other. This condition forces a relationship that fixes the direction of

$\vec{U}_{sia}$ and $\vec{U}_M$ once the low level and upper level ambient wind speeds are known in fixed coordinates (the line along which the vectors act is fixed). Since the fixed coordinate velocities are given by

$$\vec{V}_M = \vec{U}_M + \vec{\mathcal{C}} \tag{2.9}$$

and

$$\vec{V}_{sia} = \vec{U}_{sia} + \vec{\mathcal{C}} \tag{2.10}$$

then the condition

$$\vec{U}_M - \vec{U}_{sia} = \vec{V}_M - \vec{V}_{sia} \tag{2.11}$$

fixes the alignment of flow of $\vec{U}_M$ and $\vec{U}_{sia}$. (See sketch of vectors in Figure 2.7.)

We now consider $\mathcal{G}$, the mass of air taken into the storm per unit time, as

$$\mathcal{G} = \frac{\pi}{4} \rho_{sia} w D^2 \tag{2.12}$$

where w is a function of the temperature lapse rate in the middle layer air and is related to the mean upward velocity of air. Thus equation (2.8) becomes

$$0 = w D^2 K \vec{U}_{sia} + \vec{U}_M \left| \vec{U}_M \right| hD \tag{2.13}$$

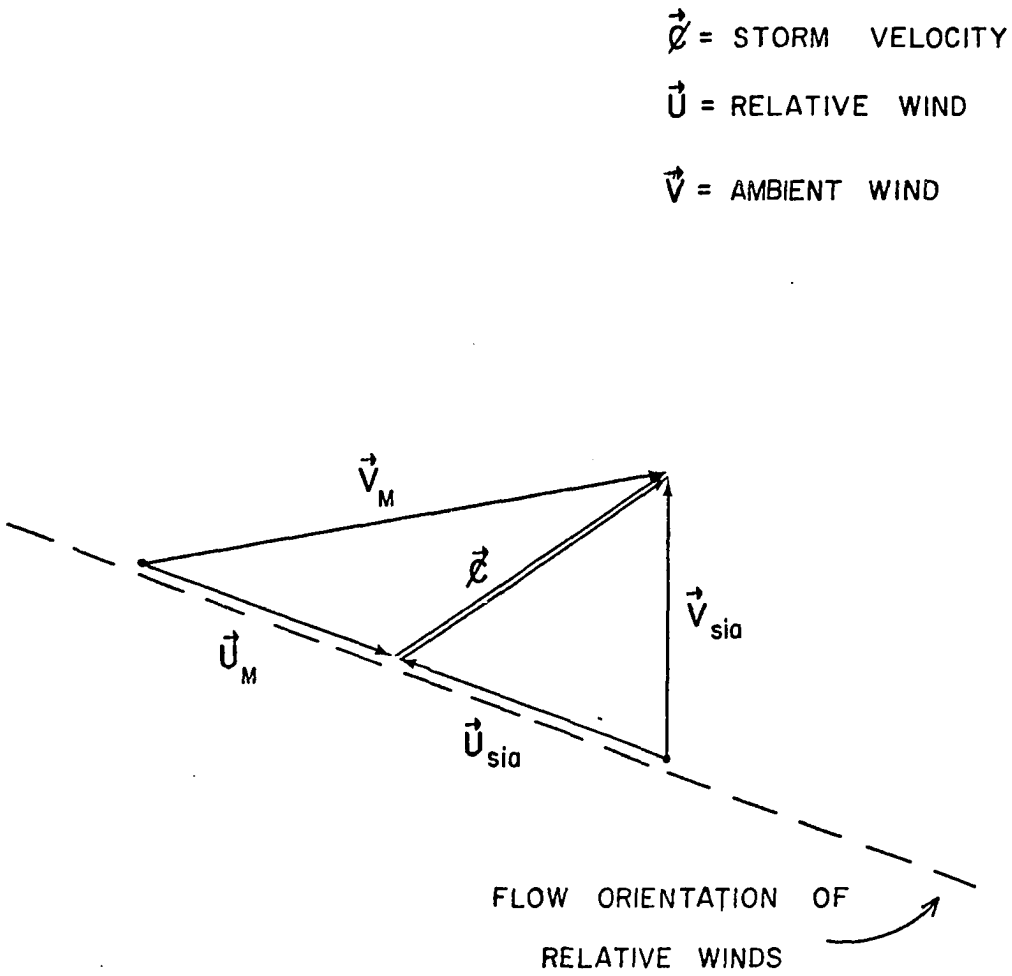

Figure 2.7 Sketch of the relation between ambient wind, $\vec{V}$, and relative wind, $\vec{U}$. Storm motion, $\vec{\mathcal{C}}$, beginning at any point along the dashed line, determines $\vec{U}_M$ and $\vec{U}_{sia}$.

We now define

$$K \equiv \frac{2\rho_{sia}}{C_D \rho_M} \cdot \frac{\pi}{4} \tag{2.14}$$

where ρ_{sia}, ρ_M are the average density for the sub-inversion layer and middle layer respectively, and C_D is the drag coefficient.

By this definition of K, we require that w represent the mean mass weighted upward flux of air in the storm.

With the direction of $\vec{U}_M$ and $\vec{U}_{sia}$ shown to be parallel, and the directions of the relative flows determined by the storm motion and the ambient flow, all directions can be determined. We now dispense with the vector notation and consider the magnitude (scalar) of the combination of the middle level with lower level flow.

Let P represent the magnitude of the difference of measurable quantities in the atmosphere,

$$P \equiv V_M - V_{sia} \tag{2.15}$$

and from (2.11)

$$U_M = U_{sia} + P \tag{2.16}$$

substituting into (2.13) we have

$$KwD\ U_{sia} + (U_{sia}^2 + 2P\ U_{sia} + P^2\ )\ h = 0 \tag{2.17}$$

Let

$$\gamma \equiv \frac{KwD}{2h} \tag{2.18}$$

then in equation (2.17)

$$U_{sia}^2 + 2U_{sia}(\gamma + P) + P^2 = 0 \tag{2.19}$$

Solving the quadratic equation of (2.19) yields

$$U_{sia} = -(\gamma + P) \pm \sqrt{2\gamma P + \gamma^2} \tag{2.20}$$

If

$$P > -\frac{\gamma}{2}$$

the radical becomes negative, which can be interpreted as an impossible condition. This results in the condition that the lower flow is greater than the middle level flow by

$$U_{sia} > U_M + \frac{KwD}{4h} \tag{2.21}$$

Evaluating K for the real atmosphere where the air density at the top of the troposphere is about one half its surface value, we estimate the ratio of densities

$$\rho_M = \frac{3}{4}\rho_{sia} \tag{2.22}$$

then from (2.14)

$$K \cong \frac{2}{C_D} \tag{2.23}$$

and for a cylindrical body

$$0.4 \leq C_D \leq 1 \tag{2.24}$$

The inward flux of air below the inversion is given by

$$J_i = \rho_{sia} \ell Z U_{sia} \tag{2.25}$$

where the ρ_{sia} and U_{sia} represent the mean density and relative velocity of the sub-inversion air that is converged upward into the storm, ℓ is the width of the channel of this air, and Z is the inversion height which represents the depth of the inflowing air.

The upward flux inside the storm is represented by

$$J_u = \rho_M \frac{\pi}{4} D^2 w \tag{2.26}$$

where ρ_M is the mean air density of the middle layer, D is the diameter of the upward motion, and w is the mean mass weighted velocity of the upward motion. This relation is illustrated in Figure 2.8.

Consider an example where

$$w = 10 \text{m sec}^{-1}$$

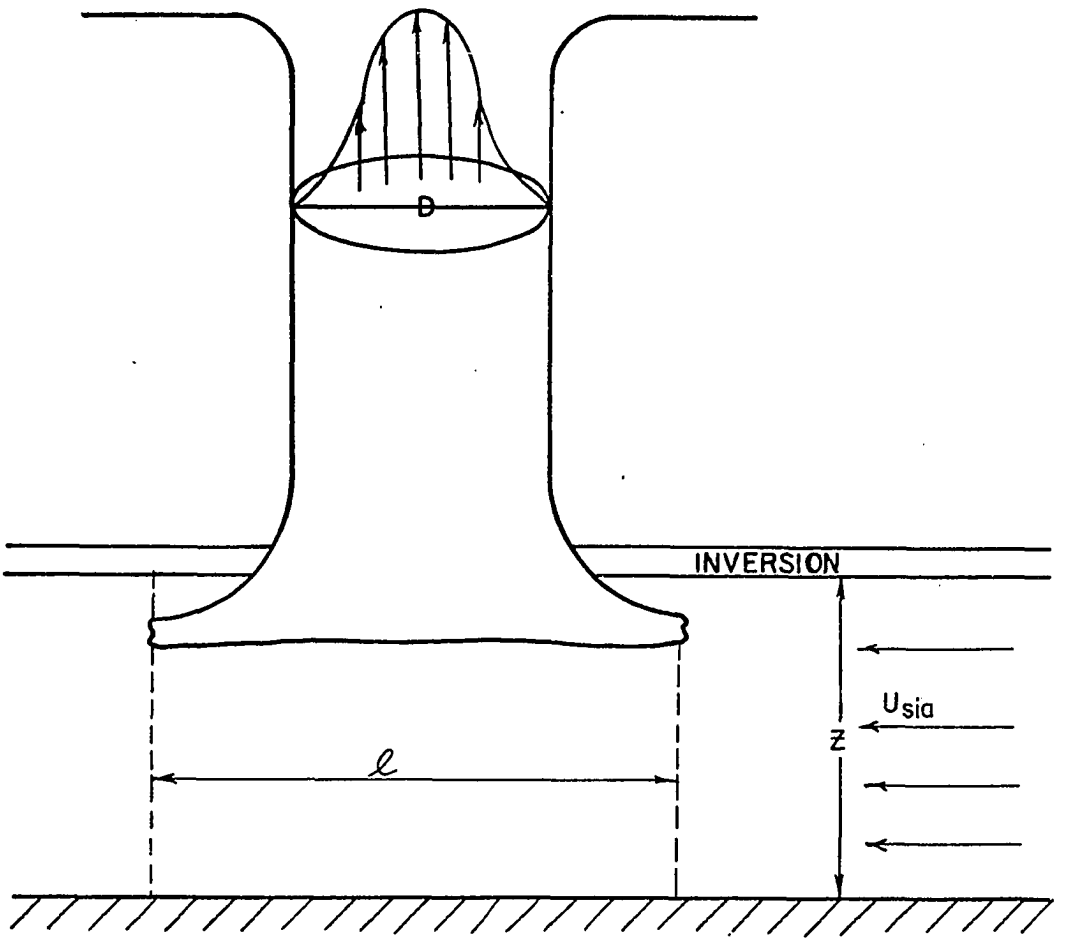

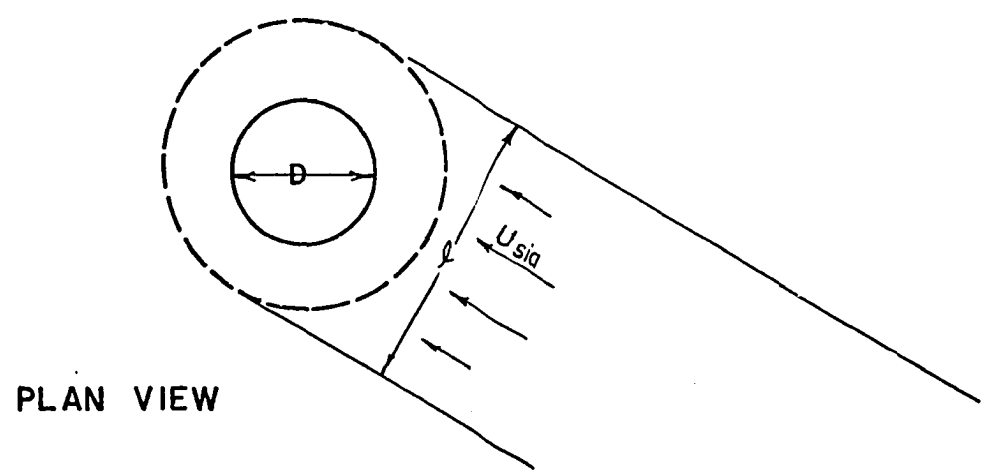

Figure 2.8. The inward flux of sub-inversion air (plan view) and the vertical flux of storm air (side view).

and where the ratio of diameter to height is within the range

$$1 \leq \frac{D}{h} \leq \frac{1}{2}$$

From (2.18) and (2.23)

$$\gamma = \frac{w}{C_D} \frac{D}{h} \qquad (2.27)$$

then from (2.24) the range in γ is given by

$$5 \text{ m sec}^{-1} \leq \gamma \leq 25 \text{ m sec}^{-1}$$

In the atmosphere storm clouds can have diameters (D) as large as 20 km and can extend to heights of 20 km. The height of the top of the inversion, Z, is usually below 2 km. Although the width, ℓ, of the channel of inflow has not yet been measured, consideration of continuity of flow into the storm suggests that ℓ be at least as large as the diameter of the cloud at its base. Therefore we assume:

$$D = 5 \text{ km}$$

$$h = 10 \text{ km}$$

$$Z = \frac{3}{2} \text{ km}$$

$$\ell = 2D$$

For the limiting drag coefficients and diameter to depth ratios, the values of the middle layer flows (U_M) are computed using equation (2.21) and,

in units of m sec^{-1}, are

$$U_{sia} > U_M + \frac{5}{2}$$

for $\frac{D}{h} = \frac{1}{2}$, $C_D = 1.0$* (2.28)

$$U_{sia} > U_M + \frac{25}{2}$$

for $\frac{D}{h} = 1$, $C_D = 0.4$* (2.29)

The restricting cases of middle level winds as a function of selected lower level relative winds are computed from equations (2.28) and (2.29) and the results are shown in Table 2.1.

TABLE 2.1

Ratio of non-allowed values of middle level relative winds U_M, to lower level winds U_{sia}

C_D \ D/h	1/2	1/1
0.4	$< \frac{4.0}{10.0}$	$< \frac{7.5}{20.0}$
1.0	$< \frac{7.5}{10.0}$	$< \frac{15.0}{20.0}$

As is shown, with the conditions of D/h = 1/2 and $C_D = 0.4$, for a lower level wind of 10 m sec^{-1} the upper level wind cannot be less than 4 m sec^{-1} and retain a constant storm speed.

* The range in drag coefficients is taken from Hoerner (1958).

In order for realistic estimates of velocities to be made, the continuity of mass must be satisfied. To satisfy this requirement (2.25) and (2.26) must be equal. Thus

$$U_{sia} = \frac{\rho_M}{\rho_{sia}} \frac{\pi}{4} \frac{D^2}{\ell Z} w \qquad (2.30)$$

If we assume that for cumulus (Cu) clouds

$D \sim \ell$, with D the order of km

and for towering cumulus or cumulonimbus (Cb) clouds

$2D \sim \ell$, with D the order of 10 km

and for both Cu and Cb

$$Z = \frac{3}{2} \text{ km}$$

and

$$\rho_M = \frac{3}{4} \rho_{sia},$$

then for Cu, equation (2.30) becomes

$$U_{sia} = \frac{\pi}{8} w \qquad (2.31)$$

and for towering Cu and Cb, equation (2.30) becomes

$$U_{sia} = 5\frac{\pi}{8} w \qquad (2.32)$$

Thus from considering the continuity requirements of the model and testing the results on cumulus and cumulonimbus clouds, a function of the mean mass weighted velocity (w) can be substituted for relative velocity of the inward air flow in the first term of the acceleration equation.

III - THE APPLICATION OF MODELED STORM MOTION

Most severe storms whose circulation may be computed from either circulating radar elements, chaff trajectories, or other means have some change in environmental wind direction with height.

Figures 3.1 and 3.2 are taken from the Browning and Fujita (1965) analysis of a group of severe storms with circulation. Path curvature is prominent in Figure 3.1. Figure 3.3 is the vertical distribution of wind at the time of initial radar echoes. The wind is both veering and shearing with height during the early stage of development of severe storms. Figure 3.2 shows the tracks of the echoes prior to 1500 CST, during their early development stage. Although difficult to see, there is some curving of the path during this early time.

Achtmeyer's study (1969) of severe storms exhibiting circulating elements also contained an environment that veered and sheared with height. Both his extrapolated wind soundings (Figure 3.4a) and his actual rawinsonde (Figure 3.4b) for that time show a marked increase in speed and a clockwise change in direction with height. Most of the radar echoes had paths (Figure 3.5) that were curved during the initial part of their trajectories.

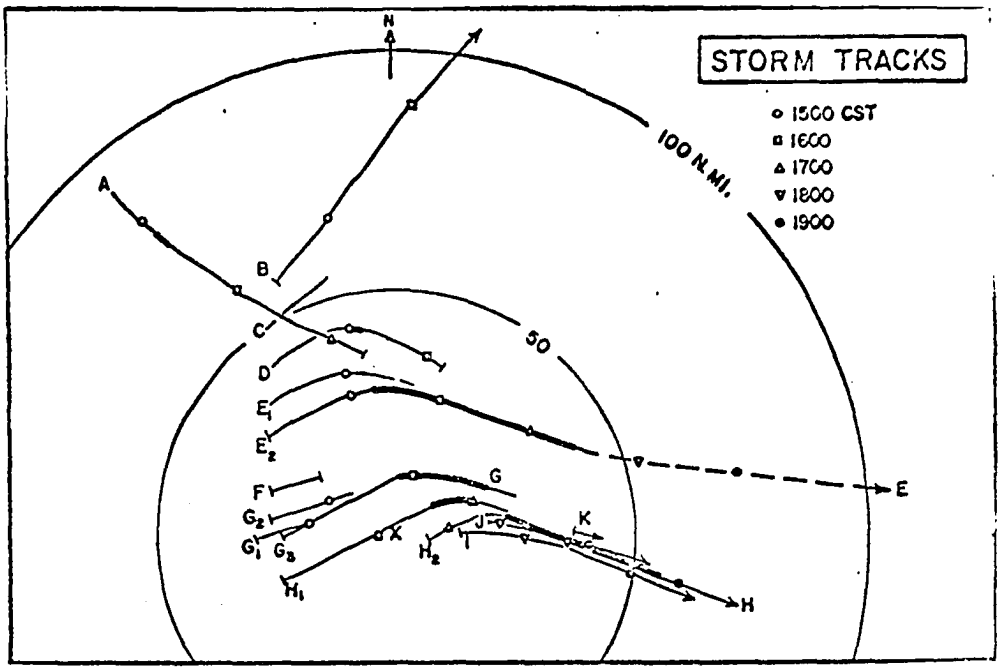

Figure 3.1 Tracks of storms A through K, derived using data from the WSR-57 radar at WRL, at the center of the range rings. Tracks of severe storms with hook echoes are denoted by thick lines. (After Browning and Fujita, 1965).

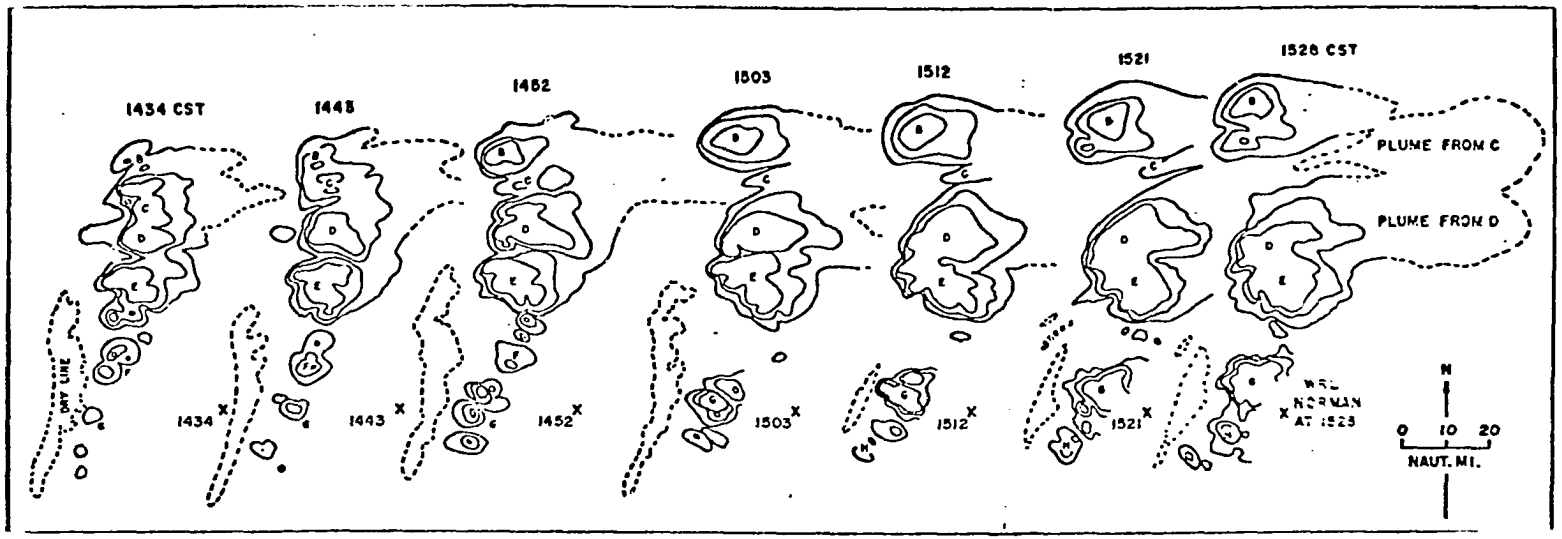

The line of storms B through H at roughly 9-min. intervals, as seen by the WRL, Norman, The position of the radar is indicated by a cross. The three solid contours, representing storm echoes at an elevation of 2^0 are for 10 $\log Z_e$ = 3, 21, 33, respectively, at a range of 30 naut. mi., where Z_e is the equivalent reflectivity factor in mm^6m^{-3}. The dashed contours represent the dry line.

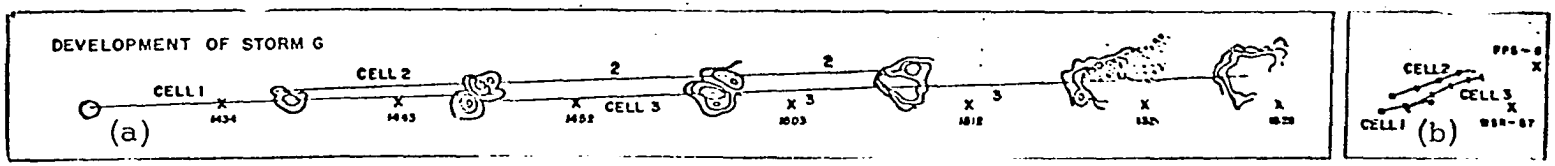

(a) Same as above but showing only the three cells comprising Storm G. Lines are drawn connecting the center of each cell from one time to the next. The shaded area depicted at time 1521 shows the time-integrated extent of hail in the surface due to Storm G during its development phase. (b) Tracks of the centers of the Storm G cells.

Figure 3.2 Radar tracks of storm cells. (After Browning and Fujita, 1965).

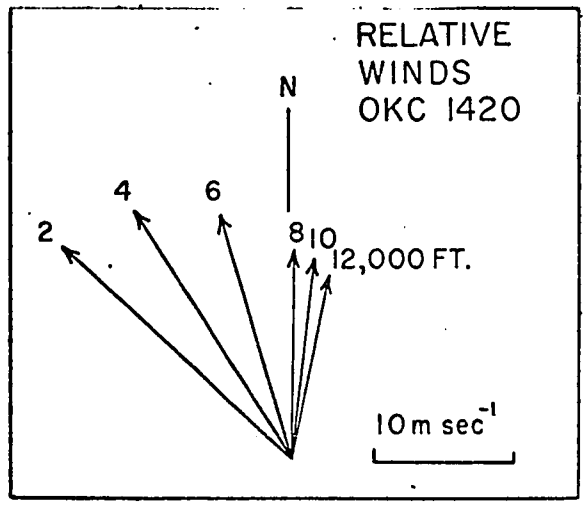

Figure 3.3. Vertical distribution of wind at initial time of radar echoes. (After Browning 1965).

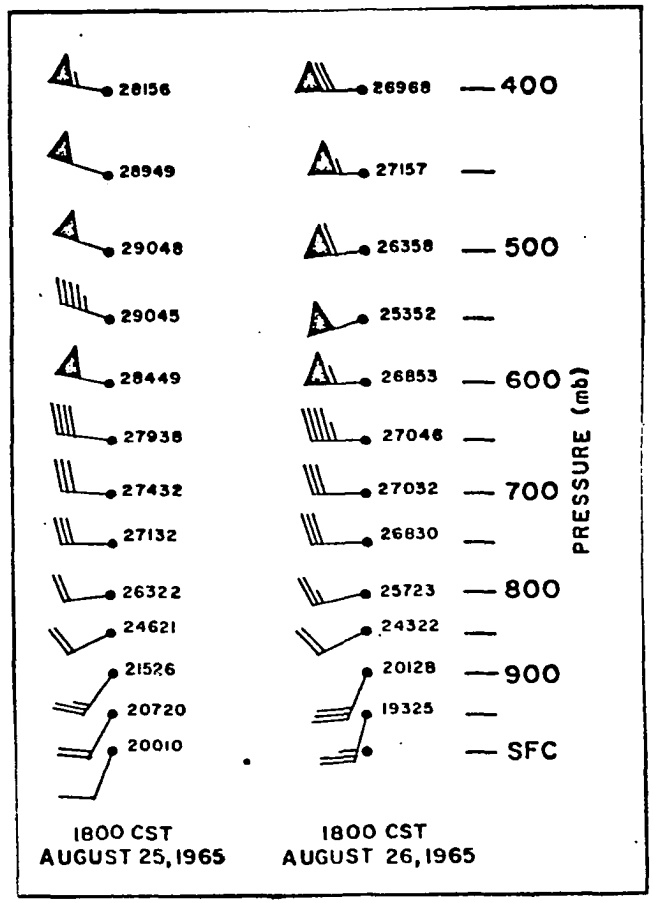

Figure 3.4a Winds extrapolated from nearby rawinsonde stations. (After Achtmeyer, 1969a).

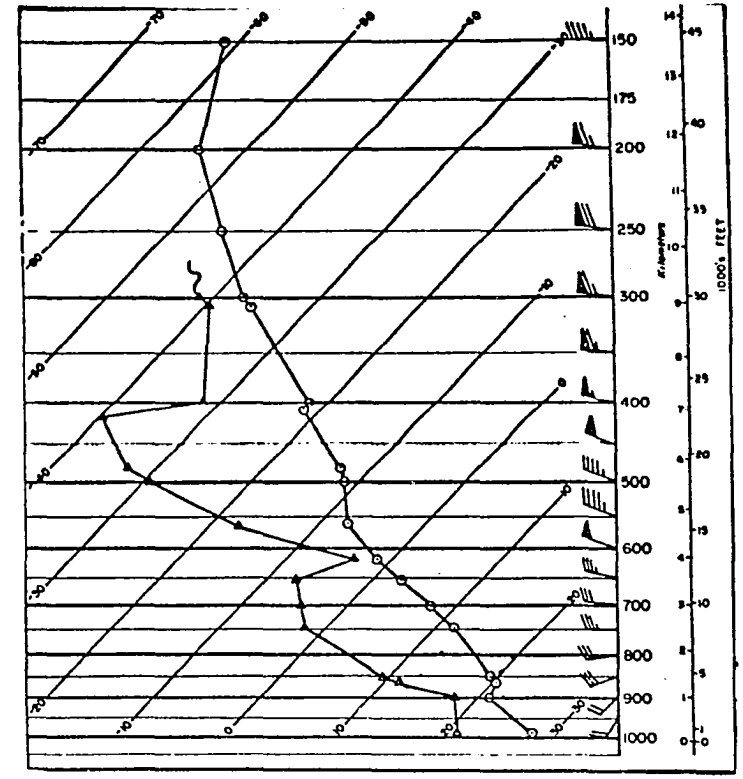

Figure 3.4b Rawinsonde observation at Peoria, Ill. at 1800 CST, 25 August 1965, illustrating the vertical distribution of temperature, dew point, and wind velocity. (After Achtmeyer, 1969b).

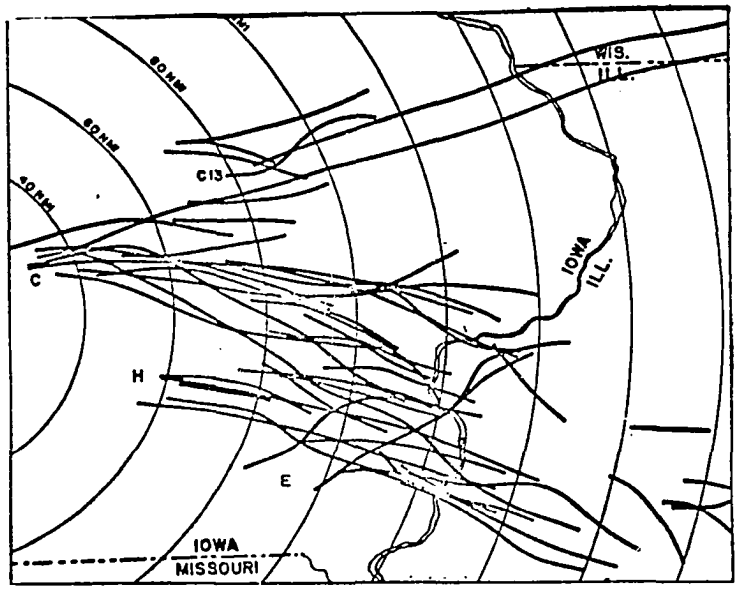

Trajectories of 72 group B radar echoes observed between 1530 and 2100 CST, 25 August 1965.

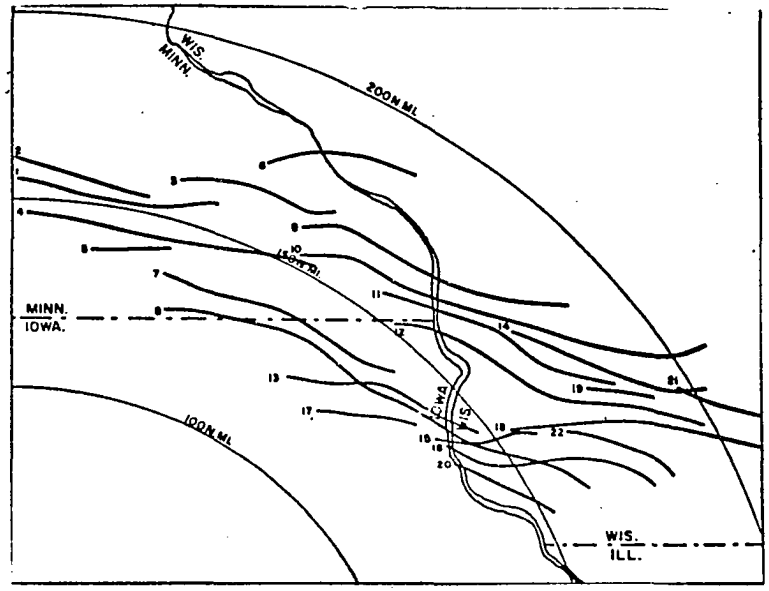

Trajectories of 22 group A radar echoes observed between 1500 and 2100 CST, 25 August 1965.

Figure 3.5. Trajectories of radar echoes. (After Achtmeyer, 1969b)

There is an inherent difficulty in trying to verify path curvature using radar during the early growth and development stage of a storm. Since the radar detectable drop sizes are usually developed after about 10 minutes of storm growth, there remains less than 20 minutes, according to our assumption, during which the storm attains its more westerly motion. For the anticyclonically curved path length of 18 km, the lesser amount of curving path occurs during the latter 12 km of the storm's history. Since most radar displays are at 20 to 50 mile range marks, the resolution needed to discern whether the 12 km path is curved or straight is most difficult unless the storm path has already begun to respond to transverse forces.

Short wave length radars will detect smaller drops and thereby allow a potentially earlier time for the curved path to be detected. However, unless the radars contain a much larger than normal power output, they are unable to detect at long range, thereby decreasing the probability that the initial stage of the storm will be detected.

An example of an opportune detection by short wave length radar is contained in the case study of the square cloud. The Wichita Falls radar (SPS) detected echoes at 1305 CST at a distance of approximately 50 miles. A careful analysis of these echoes revealed an anticyclonic curving of trajectories during the storm's development stage. A composite of these echoes for approximately a two hour period is shown in Figure 3.6. Almost all of the echoes on the southern part of the line had

curved paths that coincided with the shearing and veering environment shown in Figure 3.7. The two charts correspond to 10,000 ft and 40,000 ft altitudes near the storm echoes. The storm system continued to grow and had numerous tornadoes associated with it.

Perhaps the best example of a detected curving of path was that shown in Figure 3.8, taken from the Thunderstorm Project. In this case it is clear from the echo that the storm responded to the westerly momentum, but when the surface was more exposed to the northwesterly momentum, the echo region responded to that while retaining some of its westerly momentum. Although it is not explicit in this case study how the cloud, whose base is probably below 8,000 ft, can entrain the northwesterly momentum into it and transport the momentum forward and downward, we may assume that this is either through entrainment at the periphery or by turbulent mixing at the boundaries. If it is mixing, then eddy mixing of momentum at the cloud edges will allow it to be accelerated by the ambient flow at each level and the greater diameter will serve to enhance the drag effect.

A number of case studies of early echo development have been selected for study in differing environmental veer and shear conditions. However, because of the poor resolution of the curved paths of the developing radar echoes, these cases exhibited wavy motion and could not be considered conclusive evidence that their paths curved in the manner postulated in this thesis. What is needed is a capability to measure

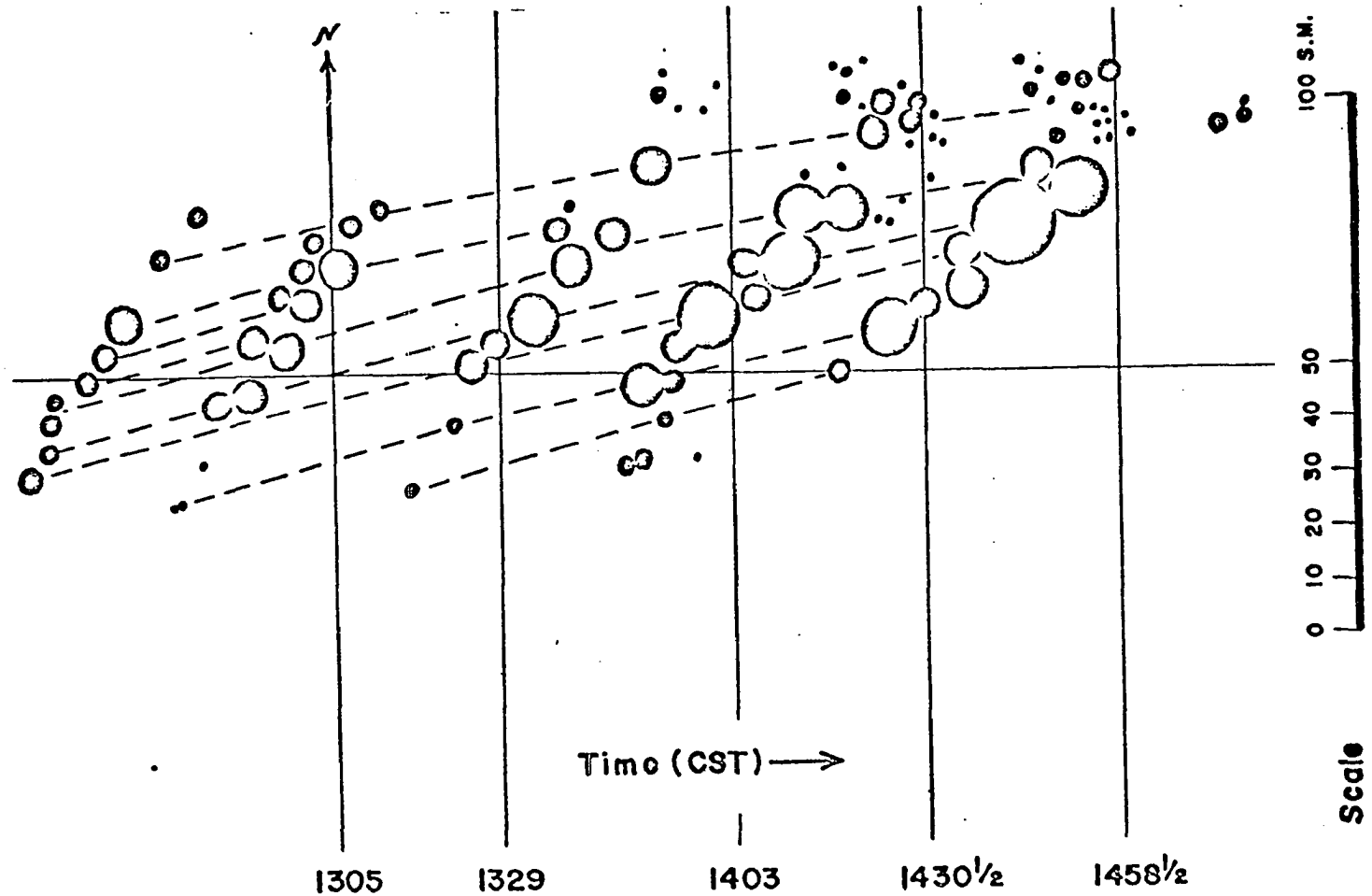

Figure 3.6. Composite time plot of the reduced SPS radar echoes. Time increases from left to right. The intersections of the horizontal with the vertical lines denote thepositions of SPS relative to the corresponding echoes. The vertical lines point to true north. Space scale is valid synoptically. (After Goldman, 1962)

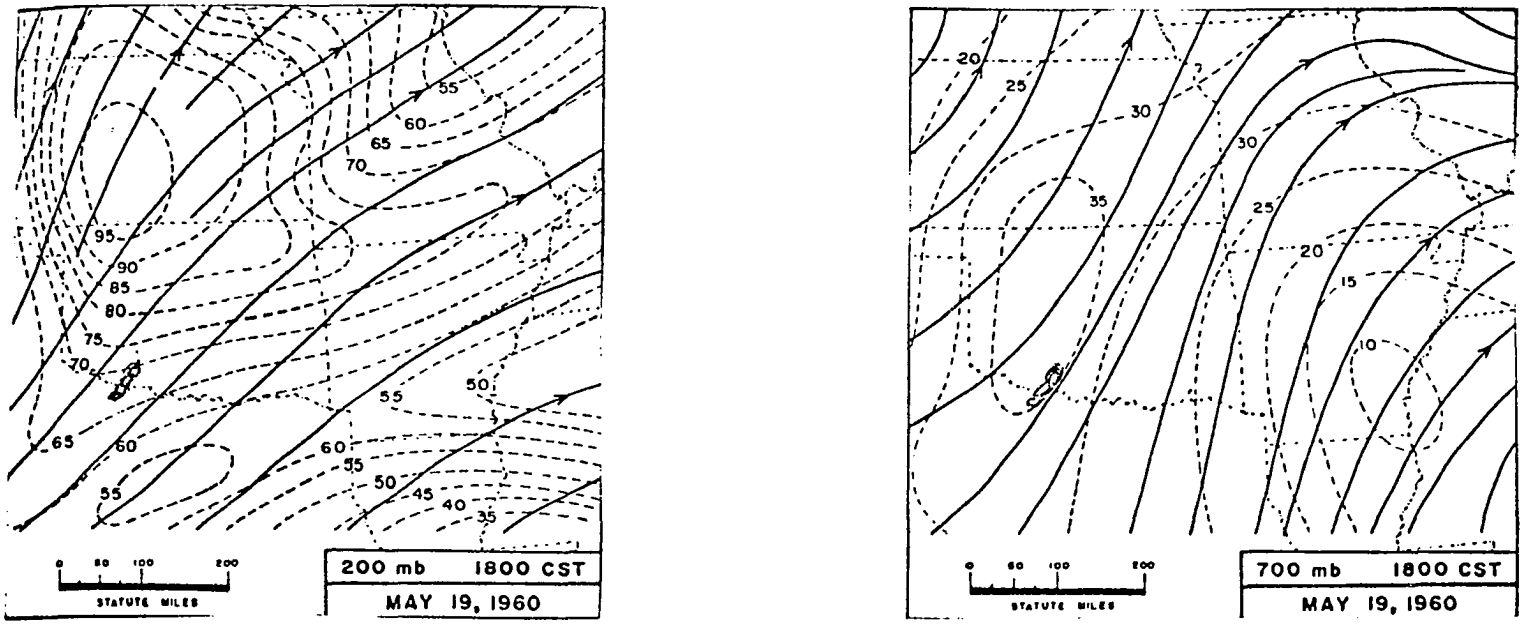

Figure 3.7 .Wind analysis for the Square-Cloud case. (After Goldman, 1962) Streamlines (solid) and isotachs (dashed lines) at 5kt intervals. SPS Radar echoes at about 1500 CST superimposed at their location on the Red River.

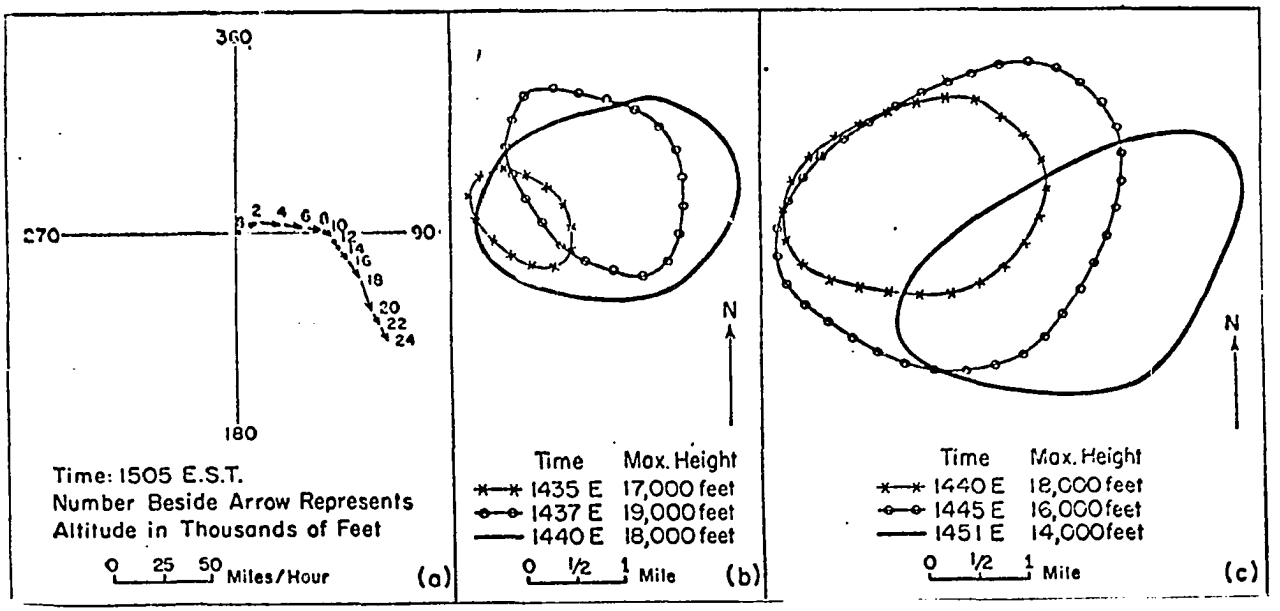

Figure 3.8. Charts showing the variation of the wind velocity with height and the change in cloud-echo movement due to the vertical transfer of horizontal momentum by the updraft and the downdraft.
(a) Wind speed and direction at each 2,000-foot level. Wind vectors are means of seven observations taken over the Ohio network. No balloon approached nearer than four miles to the radar echo.
(b) and (c) Outlines of the cross section of the radar cloud at the 5,000-foot level for successive times. The maximum height given is for the top of the echo. Note that the movement was toward the northeast during the first time interval, during which the echo was increasing its height. As the echo decreased in height, the echo moved more toward the southeast. (After Byers and Braham, 1949).

the refractive index gradients at the cloud edge and to map these gradients in three dimensions and with time. According to Atlas (private communication, 1970), this is now possible in two dimensions and time using a recently developed LIDAR with a high pulse repetition frequency. The developed unit responds to liquid water and not vapor, while leaving sufficient power and pulse repetition frequency to provide near continuous mapping capability similar to present weather radars.

IV - A CONSIDERATION OF CIRCULATION IN THE SEVERE STORM

The third term in the formulation of the acceleration of the storm (see equation 2.2) represents the circulation about the storm and its resulting transverse effects on the storm path. This chapter will be concerned with the circulation which may be induced at the periphery of the cloud due to the curvature of its path.

A. General Description

The existence of vortex circulation about severe storms in the atmosphere has been made apparent by the detailed findings of Browning and Fujita (1965). Although early investigators have recognized that severe storms such as the tornado have a large circulation associated with them, it has been only recently that the circulation has been extended to the larger scale of the cloud, to which the tornado is related. The observations and descriptions of Browning and Fujita (1965) were of a large number of severe storms that had tornadoes and giant hail associated with them. These storms occurred in the veering and shearing environment of the Great Plains, the region of maximum severe storm activity in the United States. Evidence of circulation was found in the motions of elements of the radar echo moving about the mass of storm echo at and near its edge.

Investigation such as Fankhouser's (1968) has verified that circulation exists away from the radar echo edge of severe thunderstorms. His computations of chaff trajectories, released near the storm at middle levels, show a circulation to exist about the storm at a significant distance from the cloud boundary, which should be farther than the radar echo edge. These storms were in the veering environment of the Great Plains.

Wind shear has long been recognized to be related to severe storms through large-hail formation processes. The work of Foster and Bates (1956) which culminated in a prediction method for large-size hailstones was based on wind shear. The role of wind veer was recognized and popularized by Browning and Ludlam (1962) in their study of the wind field that would support the growth of giant hailstones. They found that wind veer in the presence of wind shear would prolong the residence time of the growing hailstone. Browning later showed the wind veer to be associated with storms he studied in both England and the Great Plains of the United States.

The importance of circulation was demonstrated theoretically in Kuo's (1966) development that treated perturbation type vortices. He showed that small scale vortices, such as a tornado's, can develop from medium scale vortices, such as large storms containing circulation, in a stably stratified atmosphere with certain conditions that have been observed in the Great Plains. He showed a necessary condition for development to be the presence of an initial circulation of a scale larger than the scale

of the intense vortex.

Since both theory and observation have shown that the severe storm can and does exist in an environment containing wind veer and shear with height and circulation, it would seem likely that circulation about the storm is closely related to wind veer with height in the environment. Barnes (1968) concludes that vertical shear in the low atmosphere is a source of rotation that the storm receives through the tilting effect in the vorticity tendency equation. His conditions require a low level jet to induce vorticity, which is then tilted into the appropriate orientation so that air with this circulation can be converged toward the cloud at low levels. Tang (at the 1967 AMS-AGU Spring Meeting in Washington, D. C.) proposed a similar method of providing initial circulation; however, he used the polar jet stream to induce vorticity. Both of these methods require a mechanism that tilts the generated vortex tube and, to a lesser extent in Tang's proposal, do not require the wind to veer with height.

Although theory on the coupling of the upper and lower momenta is not yet complete, speculation leads us to couple the upper and lower flows via vertical motion. During the early stage of development, the lower level part of the storm continuously feeds the upper part that is trying to come into equilibrium with the upper level flow. This continual feeding of southerly momentum keeps the storm from moving entirely with the westerly flow aloft. To keep the bottom of the storm from being sheared off,

some of the westerly momentum from above is transported downward through the precipitation interacting with the mixture of cloud air and dry air at middle levels. The mixed air eventually becomes the cold downdraft. The westerly momentum from the middle levels is transmitted downward directly in this way; however, that momentum is very small since the wind velocity relative to the storm at middle levels is lower than the relative velocity of the upper and lower levels. It is the precipitation particles (moving horizontally with the westerly storm motion) from the upper part of the storm that transmit horizontal momentum to the middle levels inside the storm. This momentum is transmitted to the lower levels and combined with the momentum of the middle levels as the precipitation particles evaporate in the mixed air. This evaporation in the mixed air causes the air to become negatively buoyant.

1. Statement of the Problem

Does the anticyclonic curving of the path make the environment, some of which is eventually converged into the storm at low levels, have positive circulation?

2. Approach

This problem was approached using a hydrodynamic analogy to the curved path of the cloud. Assuming that the storm cloud acts as a cylindrical barrier to the flow, a cylinder was moved in a curved path, and the ensuing pattern of fluid motion revealed whether circulation was induced

in the fluid. By photographic measurement of streaklines in the fluid, both the sign of the circulation and an estimate of its magnitude can be calculated.

3. Description of the Experiment

As with all hydrodynamic experiments, sophistication of the equipment and technique can make simple experimental results seem insignificant. To avoid this, the design of this experiment was confined to that of a cylinder mounted on a swivel arm with a camera photographing streaklines, with the aid of a mirror mounted above the cylinder. The cylinder was kept from rotating by a connection with the swivel arm, thus avoiding the effect of a rotating cylinder in the fluid (i.e., the cylinder retains the same orientation with respect to a fixed direction). For convenience of design the camera was in a separate rotating frame of reference relative to the moving cylinder. Any rotation which exists in the system could be computed from the motion of a crossbar in the cylinder, since the crossbar would change orientation between photographs. Although a motor was used to achieve a constant angular velocity as the arm rotated, the short arc length of cylinder path allowed only the average angular speed of motion of the cylinder to be measured at each trial.

The resulting data was streaklines on photographs. The length of the streakline is a function of its distance from the center of rotation of the arm, and the actual length is based on the initial measurement of the cylinder diameter appearing in each photograph. The exposure time of

each photograph determined the streak length as a function of rotation speed. The difference in length of streaks about the cylinder (other than that produced by the rotating system) is a measure of the circulation.

B. Theoretical Considerations of the Experimental Analogy

The experiment contains an outside force, namely that force which gives rise to the angular velocity at the swivel. We now consider the contribution of the rotation about the swivel to the circulation about the cylinder.

As shown in Figure 4.1, for a cylinder of radius r_c at a distance $R + r_c$ from the swivel, the arc length at the closest point to the swivel is given by

$$S_1 = R\,\theta \tag{4.1}$$

where θ is the angle of rotation at the swivel.

At the farthest distance from the swivel, at $R + 2r_c$, the arc length is given by

$$S_2 = (R + 2r_c)\,\theta \tag{4.2}$$

The difference in these arc lengths, $S_2 - S_1$, is given by

$$\Delta S = (R + 2r_c - R)\,\theta = 2r_c\theta \tag{4.3}$$

Measured along the circumference of the cylinder, this is given by

$$\Delta S = r_c\,\alpha \tag{4.4}$$

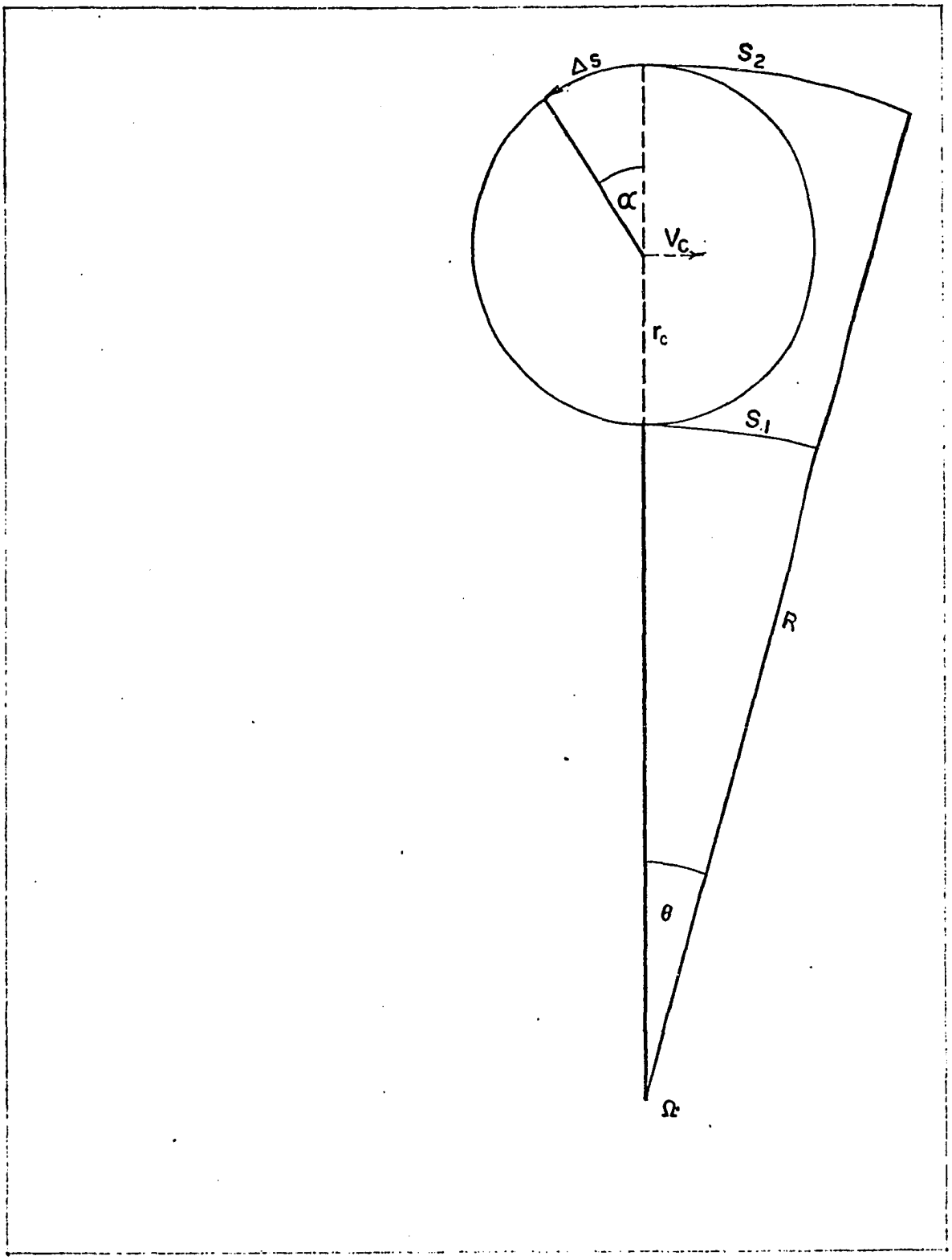

Figure 4.1. Coordinate system for moving cylinder experiments.

where α is the central angle subtended by arc ΔS.

In the direction shown in the figure (counterclockwise) ΔS is that arc length through which the cylinder would rotate in order to counter the rotation rate Ω of the swivel arm, or to remain nonrotating with respect to the center of the cylinder or any fixed coordinate system. From equations (4.3) and (4.4)

$$\alpha = 2\theta \tag{4.5}$$

The circulation about any closed path is given by the cyclic integral of the velocity, $\vec{V}$, along the path $\vec{S}$.

$$\Gamma = \oint \vec{V} \cdot d\vec{S} \tag{4.6}$$

For this circular cylinder the tangential velocity is

$$V = r_c \frac{d\alpha}{dt} \tag{4.7}$$

and the path is the circumference. Therefore

$$\Gamma = 2\pi r_c^2 \frac{d\alpha}{dt} \tag{4.8}$$

In terms of θ,

$$\Gamma = 4\pi r_c^2 \frac{d\theta}{dt} \tag{4.9}$$

The vorticity is defined as the circulation per unit area; then at the cylinder

$$\zeta = \frac{\Gamma}{\pi r^2} \tag{4.10}$$

and from equation (4.9)

$$\zeta = 4 \frac{d\theta}{dt} \tag{4.11}$$

If we prescribe the velocity of the center of the cylinder to be V_c as shown in Figure (4.1) at a distance, $R + r$, from the swivel, then the angular velocity of the swivel $\frac{d\theta}{dt}$ is given by

$$\frac{d\theta}{dt} = \frac{V_c}{R + r_c} \tag{4.12}$$

and from equation (4.11) we see that the vorticity at the cylinder

$$\zeta = 4\Omega \tag{4.13}$$

where Ω is the angular velocity at the swivel.

The vorticity at the swivel is given by

$$\zeta_s = \frac{\Gamma_s}{\pi(R + r_c)^2} \tag{4.14}$$

where Γ_s is the circulation about the swivel at the radius $(R + r)$ and is given by

$$\Gamma_s = 2\pi (R + r_c) V_c \tag{4.15}$$

Therefore the vorticity at the swivel is

$$\zeta_s = \frac{2V_c}{R + r_c} \tag{4.16}$$

Since

$$\Omega = \frac{V_c}{R + r_c} \tag{4.17}$$

the angular velocity at the swivel, then from equations (4.13) and (4.16)

$$\zeta_s = 2\zeta \tag{4.18}$$

The effect of having the cylinder remain in a nonrotating frame with respect to a fixed direction while traveling a curved path is to impart twice the vorticity of the whole system to the region about the cylinder itself.

The outside force that provides rotation about the swivel is analogous to the ambient wind that veers with height and forces the storm to move in a curved path. This path is curved anticyclonically and the vorticity that is imparted is cyclonic.

In the veering and shearing environment of the atmosphere, the storm cloud grows in both height and diameter. As shown in Figure 4.2 the ambient winds at each height level (thin arrows) affect the cloud's motion through the relative winds (bold arrows). Drag (by the relative winds that shear with height) increases as the cloud diameter increases, and the response to the drag is the curved path (shown dashed in Figure 4.2). The magnitude of the circulation induced for the indicated path of

$\pi/2$ radians arc length which occurs during the time period t_0 to t_5 can be computed if we specify the time period and the area of the cloud. The area of the growing cloud is taken at its final size after growing for an assumed time period of 30 minutes to a diameter of 10 km.

The circulation , Γ, about the curving cloud is given by its vorticity times its area. From equations (4.16), (4.17) and (4.18), we conclude that the vorticity at the cloud is 4 times the angular velocity, Ω. The circulation is given by vorticity times the area as

$$\Gamma = 4\Omega \times \frac{\pi}{4} D^2 \qquad (4.19)$$

Considering a curving of path that is represented by an arc length that is 1/3 of that shown in Figure 4.2 and which occurs during a period of 30 minutes, then the angular velocity

$$\Omega = \frac{\pi}{3 \times 3.6} \times 10^{-3} \text{ sec}^{-1}$$

For a diameter, D, of 10 km, the circulation becomes

$$\Gamma = 9 \times 10^4 \text{ m}^2 \text{sec}^{-1}$$

Circulations computed from tornadic winds, 100 m sec^{-1} at a radius of 150 meters, are approximately 10^5 m^2 sec^{-1}. Therefore the circulation induced by the curving motion is significant and comparable to tornadic storm circulation. The comparison is not presented to imply a mechanism for tornado generation, but only to show the significance of the magnitude of circulation.

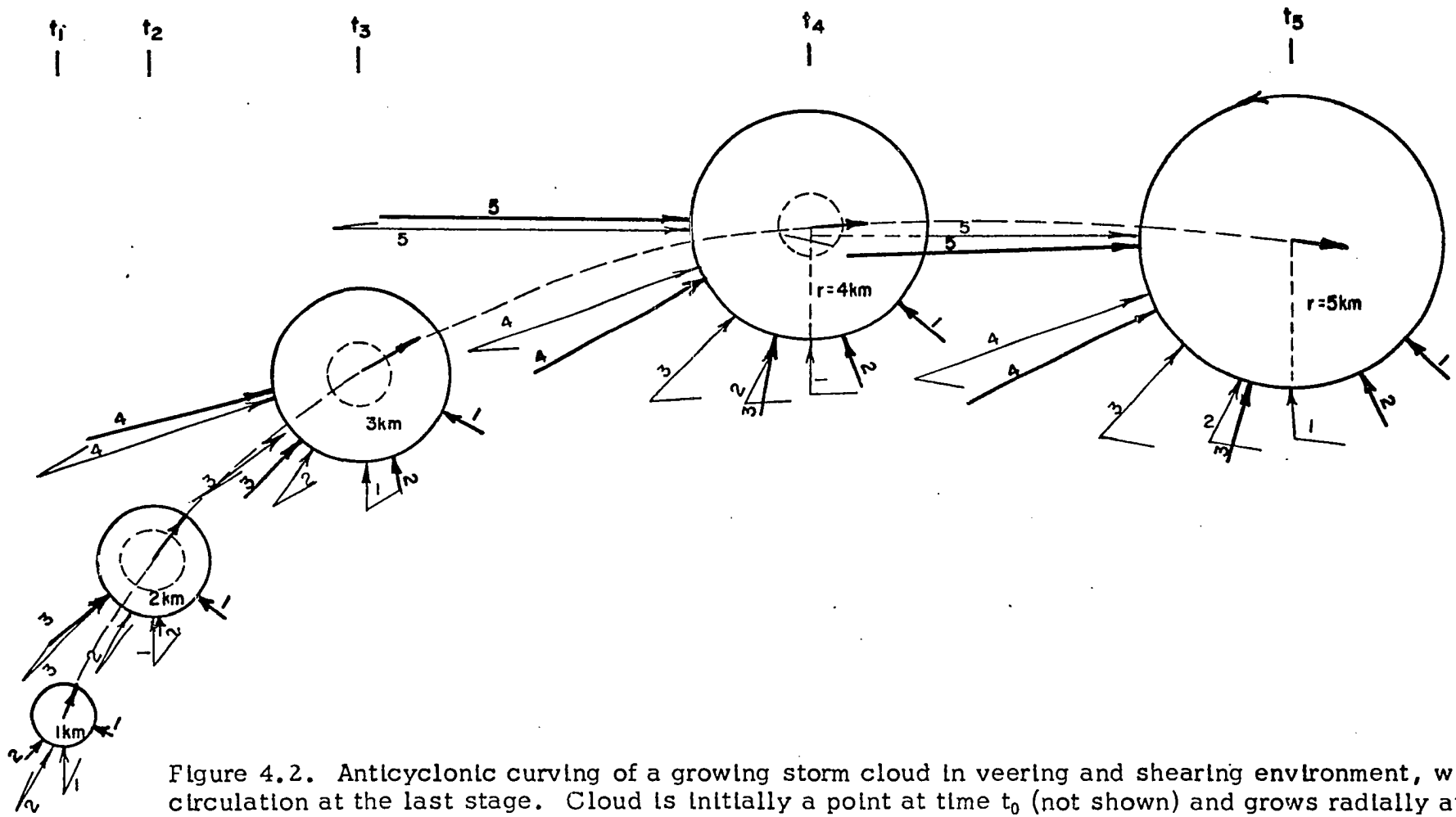

Figure 4.2. Anticyclonic curving of a growing storm cloud in veering and shearing environment, with circulation at the last stage. Cloud is initially a point at time t_0 (not shown) and grows radially at rate of 1 km per time period and vertically to level 5 by t_4. Cloud motion, indicated by arrow at center of cylinders, differs at each time as the cloud is affected by the combination of indicated winds that extend throughout its depth. Thin arrows represent ambient winds and bold arrows represent winds relative to moving storm.

C. Results of the Experiment

Photographs taken of the flow about the cylinder at varying rotation speeds indicate qualitative agreement that vorticity exists about the cylinder.

Figures 4.3 and 4.4 show streaklines with greater curvature on the side closest to the center of curvature. Some pictures show a greater number of vortices shed on the outer side, indicating a larger vortex shedding rate due to a higher velocity on that side. In these photographs the cylinder revolves about the swivel in a counterclockwise direction and, as is indicated by the crossbar, the cylinder does not rotate about its own axis.

In a previous experiment using a long cylinder a similar flow field resulted. In Figure 4.5, the cylinder is revolving clockwise about the swivel and the streaklines seem to have greater curvature on the side closest to the center of curvature.

Average tangential velocities have been recorded for each trial in both experiments. The theoretical streak lengths have been computed for each trial using the exposure time of the photograph. The lack of a more distinct tracer has precluded the measurement of streakline lengths with accuracy sufficient for computation of vorticity.

1. Data and Results of Streak Length Computations

Streak lengths were measured on photographs from three trials of the December 6, 1968 experiment. In these, as in other trials, a number of variables was measured and recorded. The average angular velocity with the clockwise, c, or counter clockwise, cc, sense of revolution about the swivel were recorded for each trial. The radius of curvature, given by the distance from the center of the cylinder to the center of the swivel, was measured and recorded at each change in length. The photograph settings of exposure time, t_e, aperature and focal length of the lense used were all recorded; however, only the exposure time was used in the calculations.

In Table 4.1 are listed measurements necessary for comparing theoretical with experimental results from three different trials.

TABLE 4.1

Measurements of experimental variables for streak length computations for experiment of December 6, 1968.

Trial Number	II	III	V
Photo Number	11	16	26
Radius of Curvature (cm)	43.1	43.1	63.5
Average Angular Velocity (sec^{-1})	0.42	0.35	0.256
Exposure Time (sec)	1/4	1/4	1/4
Enlargement Factor	1.27	1.25	1.28

Two measurements were made on the photographs: the location of the streaks and the length of the streaks. The streaks were located relative to the center of the cylinder. The distance between the center of the streaks and the perpendicular to the curved path of the cylinder was recorded with the streak length on each photograph. These measurements are listed in Tables 4.2 through 4.4 with the related computations that correct the lengths for photographic enlargement. The negative distances refer to streaks located between the cylinder's path and the center of curvature, the swivel.

The distribution of streak lengths, an example of which is shown in Figure 4.8, measured on the three photographs is far from uniform since the distinct streaks were not always distributed uniformly. The beginnings

TABLE 4.2

Theoretically computed, S_r, and experimentally measured, S, streak lengths (cm) for photo 11

STREAK NUMBER	R	R_s	r_c	r_s	S_r	S
1	43.1	39.79	2.5	7.4	5.48	5.32
2	↓	40.19	↓	5.0	5.74	5.91
3		40.46		4.9	5.77	6.09
4		41.13		8.1	5.60	5.05
5		42.23		5.7	5.72	4.27
6		44.99		4.0	5.64	5.73
7		45.78		3.8	5.48	7.08
8		46.29		4.4	5.62	9.09
9		45.82		5.3	5.78	5.82
10		46.41		4.9	5.74	5.56
11		46.80		4.6	5.64	5.89
12		47.00		4.6	5.64	5.30
13		47.74		4.7	5.65	5.73
14		48.14		8.4	6.16	4.95
15		49.00		6.4	6.06	3.60
16		50.00		7.3	6.22	3.48
17		49.67		6.6	6.14	4.84
18		49.79		7.4	6.24	6.08
19		50.70		7.6	6.35	4.03

TABLE 4.3

Theoretically computed, S_r, and experimentally measured, S, streak lengths (cm) for photo 16

STREAK NUMBER	R	R_s	r_c	r_s	S_r	S
1	43.1	39.68	2.5	6.4	4.55	7.45
2	↓	40.70	↓	7.2	4.55	6.80
3		39.74		7.4	4.50	5.95
4		39.46		5.2	4.55	6.16
5		39.98		5.0	4.71	7.42
6		40.74		4.7	4.74	6.95
7		40.02		3.7	5.00	8.00
8		41.20		4.7	4.74	6.19
9		42.14		6.4	4.65	6.00
10		44.90		5.6	4.75	6.92
11		44.74		6.8	4.79	6.50
12		46.26		7.3	4.95	4.94
13		46.62		3.7	4.38	6.85
14		45.70		6.1	4.80	8.39
15		47.34		5.9	4.84	5.24
16		47.62		4.5	4.56	6.01
17		47.98		7.2	4.98	5.95
18		48.46		5.7	4.84	5.58
19		48.34		5.5	4.80	5.05
20		47.86		7.6	5.01	4.80
21		49.14		8.8	5.15	6.48
22		50.06		7.3	5.15	5.55
23		49.70		7.6	5.13	6.30

TABLE 4.3
(cont.)

STREAK NUMBER	R	R_s	r_c	r_s	S_r	S
24	43.1	50.66	2.5	10.1	5.34	5.00
25	↓	50.82	↓	9.4	5.32	5.83
26		51.02		8.3	5.26	4.97
27		50.92		8.0	5.25	4.00
28		51.06		10.0	5.36	7.05

TABLE 4.4

Theoretically computed, S_r, and experimentally measured, S, streak lengths (cm) for photo 26

STREAK NUMBER	R	R_s	r_c	r_s	S_r	S
1	63.5	61.35	2.5	4.61	5.25	6.90
2	↓	59.95	↓	5.00	5.20	6.60
3		60.22		3.32	5.30	5.80
4		61.99		6.28	5.67	7.95
5		61.08		5.82	5.15	8.03
6		64.42		4.84	5.20	4.08
7		65.96		4.77	5.17	4.95
8		66.12		5.93	5.19	3.83
9		67.39		4.37	5.10	5.67
10		68.76		8.16	5.45	4.00
11		68.85		5.55	5.28	6.54
12		67.97		4.49	5.13	6.21
13		69.43		5.93	5.33	4.97
14		68.80		7.41	5.43	6.22
15		71.04		7.75	5.57	4.98
16		70.52		7.07	5.49	5.20
17		70.98		7.70	5.55	4.75
18		72.37		9.80	5.73	6.15
19		71.68		8.95	5.66	4.85

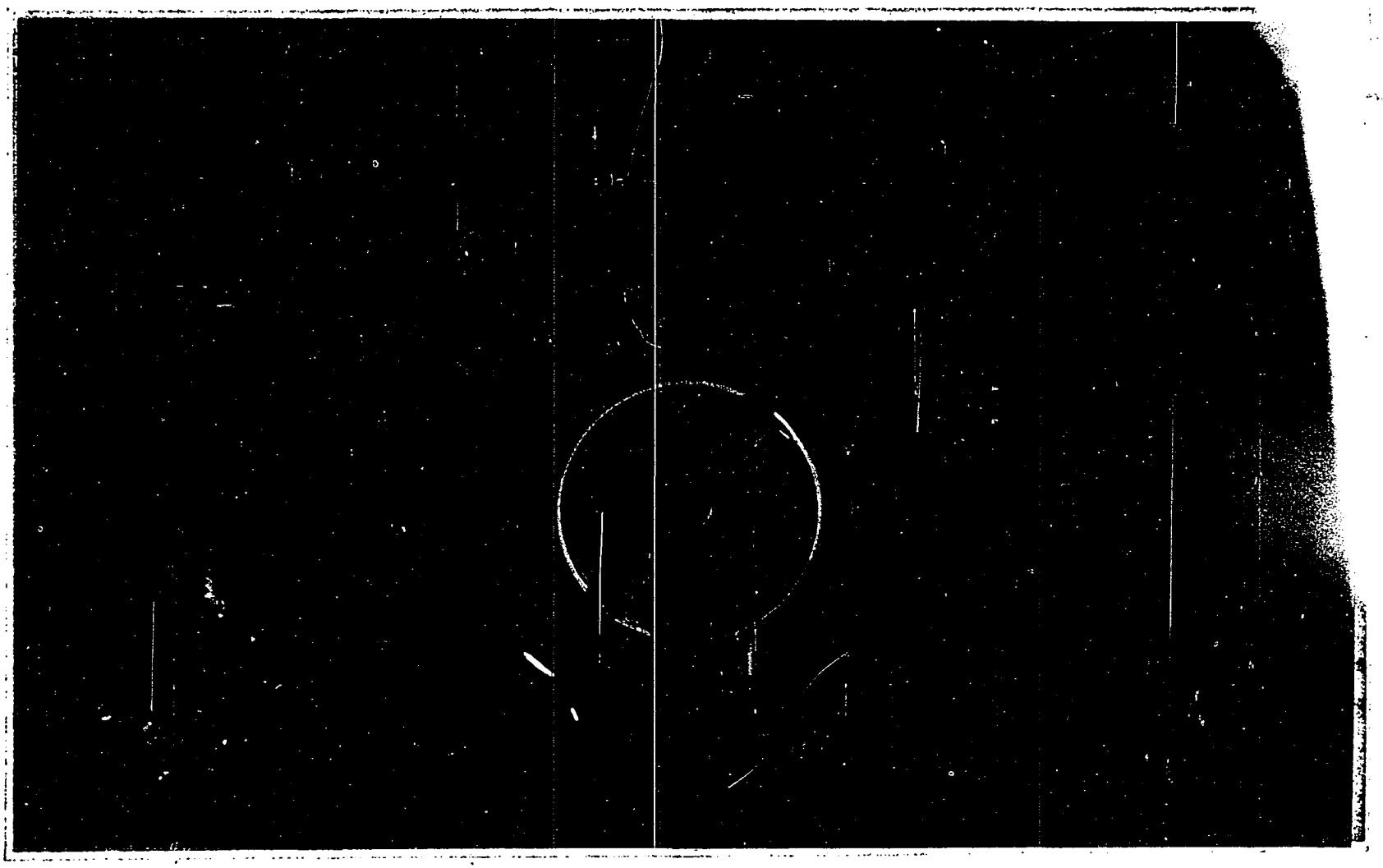

Figure 4.3. Results of second curving cylinder experiment. Photograph of motion relative to the cylinder on a path of constant curvature. Streak lines formed by aluminum powder tracer. Cylinder extends from near the bottom of the channel to above the surface. Cylinder motion from right to left.

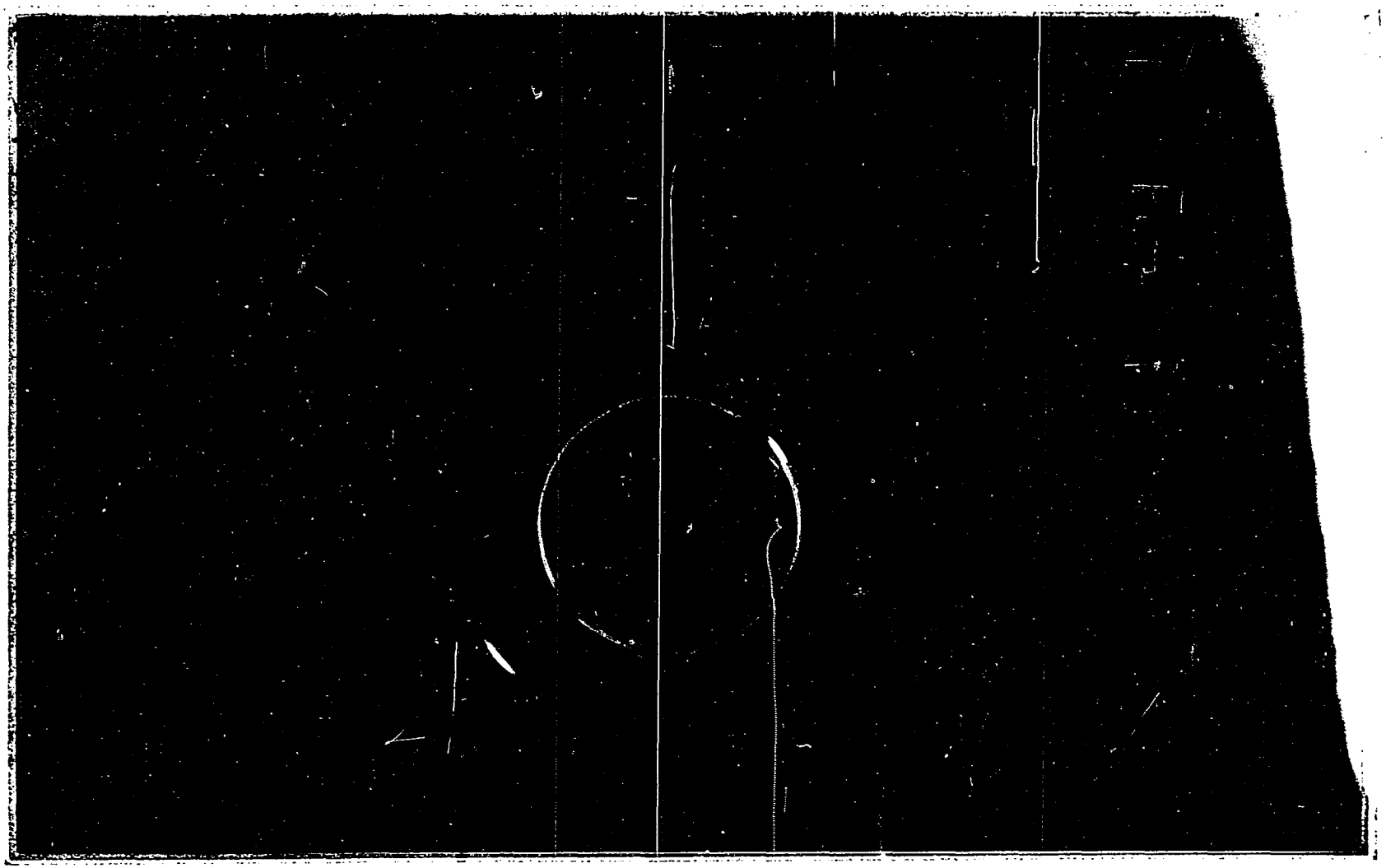

Figure 4.4. Results of second curving cylinder experiment following Figure 4.3 at same trial (taken approximately 1/2 second later). Cylinder motion from right to left.

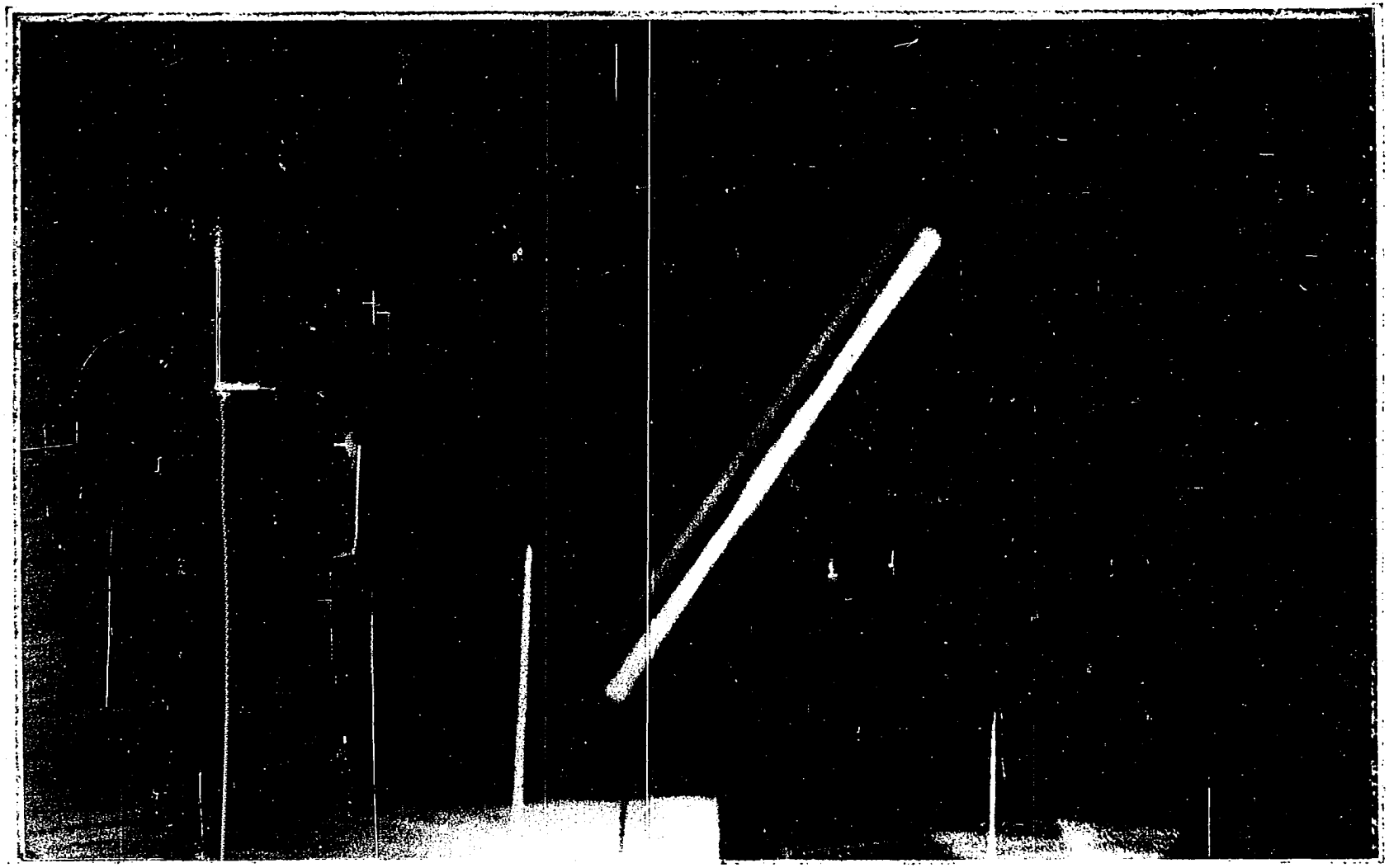

Figure 4.5 Results of first successful curving cylinder experiment. Same experimental set up except for the longer cylinder (which obscured most of the boundary layer flow) and larger tracer elements. Cylinder motion from left to right. Note the resemblance in streakline curvature to the clockwise motion about the swivel.

and endings of the streaks were highly dependent on judgement, making their measurements far from the accuracy desired for establishing quantitative relations.

In Figure 4.6 the length of the streaks is plotted against their locations with respect to the cylinder path. The location is measured as the distance from the curved path to the middle of the streaks with negative values for streaks that are located between the cylinder and the swivel.

The points on the streak length vs. distance diagrams were scattered. If we fit a straight line between the scatter of points and the center of curvature, where the streak length is theoretically zero, we find that the points at negative distances (indicating a location between the cylinder and the center of curvature) are generally displaced above the line indicating they have generally larger streak lenghts. This is definitely true for two of the pictures while the third shows the straight line slope to represent almost all the points.

The theoretical streak lengths were derived assuming that the measured streak length is the result of two contributions, the rotation of the system about the swivel and the circulation about the cylinder.

As shown in Figure 4.7, the contribution due to the tangential motion about the cylinder, S_ω, is given by the product of the tangential velocity about the cylinder, V_θ, and the exposure time, t_e. The contributions due to motion of the cylinder about the swivel, S_Ω, is given by

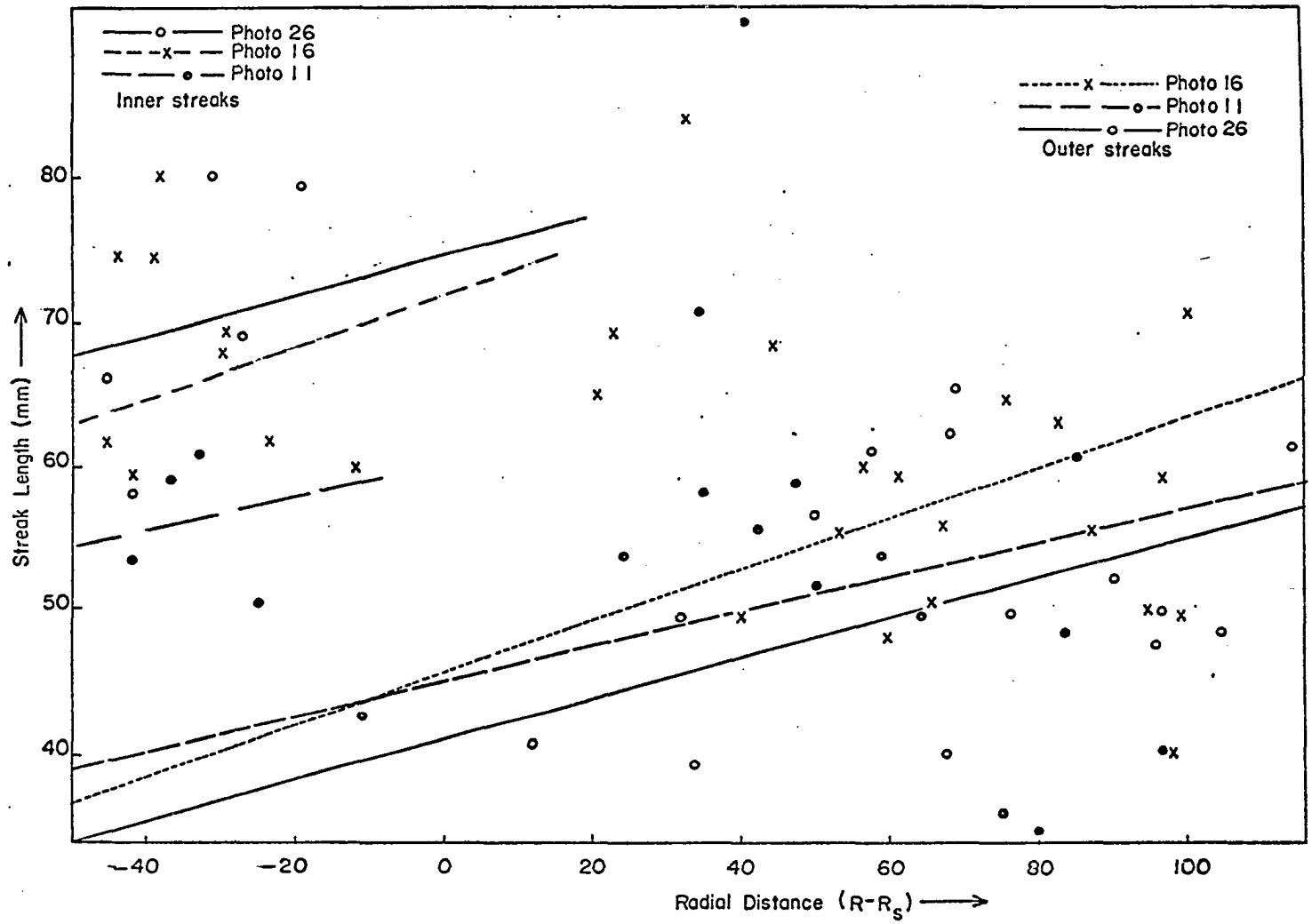

Figure 4.6 Plot of measured values of streak length vs distance from the swivel, R_s. R is the distance from the swivel to the cylinder center. Negative values of $R - R_s$ indicate locations between the cylinder and the swivel. Note, generally larger streak lengths at these locations.

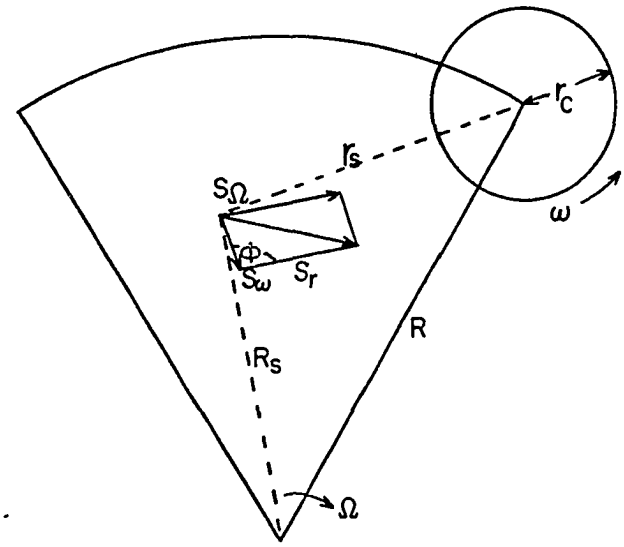

Figure 4.7 Geometry of the contribution to streak length, S_r, due to circulation about the cylinder and rotation about the swivel. ϕ is the angle between the components, S_ω, due to the circulation about the cylinder, and, S_Ω, due to the rotation about the swivel. R_s and r_s are the radial distances to the streaks from the swivel and cylinder, respectively.

the product of the tangential velocity, $V_{\theta s}$, due to rotation about the swivel and the exposure time, t_e.

The tangential velocity of any point about the swivel is given by

$$V_{\theta s} = R_s \Omega \tag{4.20}$$

where R_s is the distance from the point (in this case the midpoint of the streaks) to the swivel.

Then the contribution to the streak length by the motion about the swivel is given by

$$S_\Omega = R_s \Omega t_e \tag{4.21}$$

If the cylinder imparts circulation to the environment, then the imparted circulation measured at a distance from the cylinder edge cannot be greater than the amount that would result from the conservation of angular momentum. We assume that the contribution to streak length made by the induced circulation decreases inversely with distance from the cylinder.

The circulation at the cylinder edge is related to the tangential velocity, V_θ, at a distance, r, from the center of the cylinder by

$$\omega r_c^2 = r V_\theta \tag{4.22}$$

where ω is the angular velocity at the cylinder of radius r_c, which was

shown to be equal to four times the angular velocity at the swivel, Ω.

Then the contribution of the circulation around the cylinder to the streak length in the proximity of the cylinder is

$$S_\omega = \frac{r_c^2}{r_s} \omega t_e \tag{4.23}$$

where r_s is the distance from the streak's midpoint to the center of the cylinder.

The contributions are combined vectorially as shown in Figure 4.7 to yield the theoretical streaks length, S_r, as

$$S_r = (S_\Omega^2 + S_\omega^2 - 2 S_\Omega S_\omega \cos \phi)^{1/2} \tag{4.24}$$

where ϕ is the angle described by the two radii r_s and R_s at the midpoint of the streaks as seen in Figure 4.7.

After substituting from equations (4.21) and (4.23) in terms of Ω while considering the law of cosines, equation (4.24) reduces to

$$S_r = \Omega t_e \left[R_s^2 + 16 \frac{r_c^4}{r_s^2} - 4 \frac{r_c^2}{r_s^2} (r_s^2 + R_s^2 - R^2) \right]^{1/2} \tag{4.25}$$

Results of computations of theoretical streak length S_r using equation (4.25) are shown in Tables 4.2 through 4.4. The measured values, after accounting for photographic enlargement, are also listed for comparison.

In Figure 4.8 the theoretical and experimental values are plotted to the left and right, respectively, of the point representing the midpoint of the streak. Each streak is numbered and the values correspond to the tabulated values for each plot.

The measured streak lengths are considerably larger than would be expected if the fluid were responding only to rotation about the swivel. Also, the percent increase in streak length near the cylinder, progressing toward the swivel (toward the bottom, in the figure), generally approximates the percent increase in the theoretical streak lengths in that direction (see e.g. streaks 1 through 14). There is no doubt that the measured streaks are larger toward the swivel side of the cylinder (the bottom side in the figure). Photographs 11 and 26 show the general distribution but contain fewer measureable streaks.

The values computed theoretically contain no allowance for frictional loss of circulation in the fluid. The values are therefore considered high and are expected to be greater than measured streak lengths. However, since the experimental values of streak lengths measured on the photographs are generally higher than the corresponding theoretical values, the difference is attributible to difficulties in determining distinct streak beginnings and endings.

The difference between measured and theoretical values is generally about 20 percent. Future refinements in experimental techniques are expected to reduce that difference.

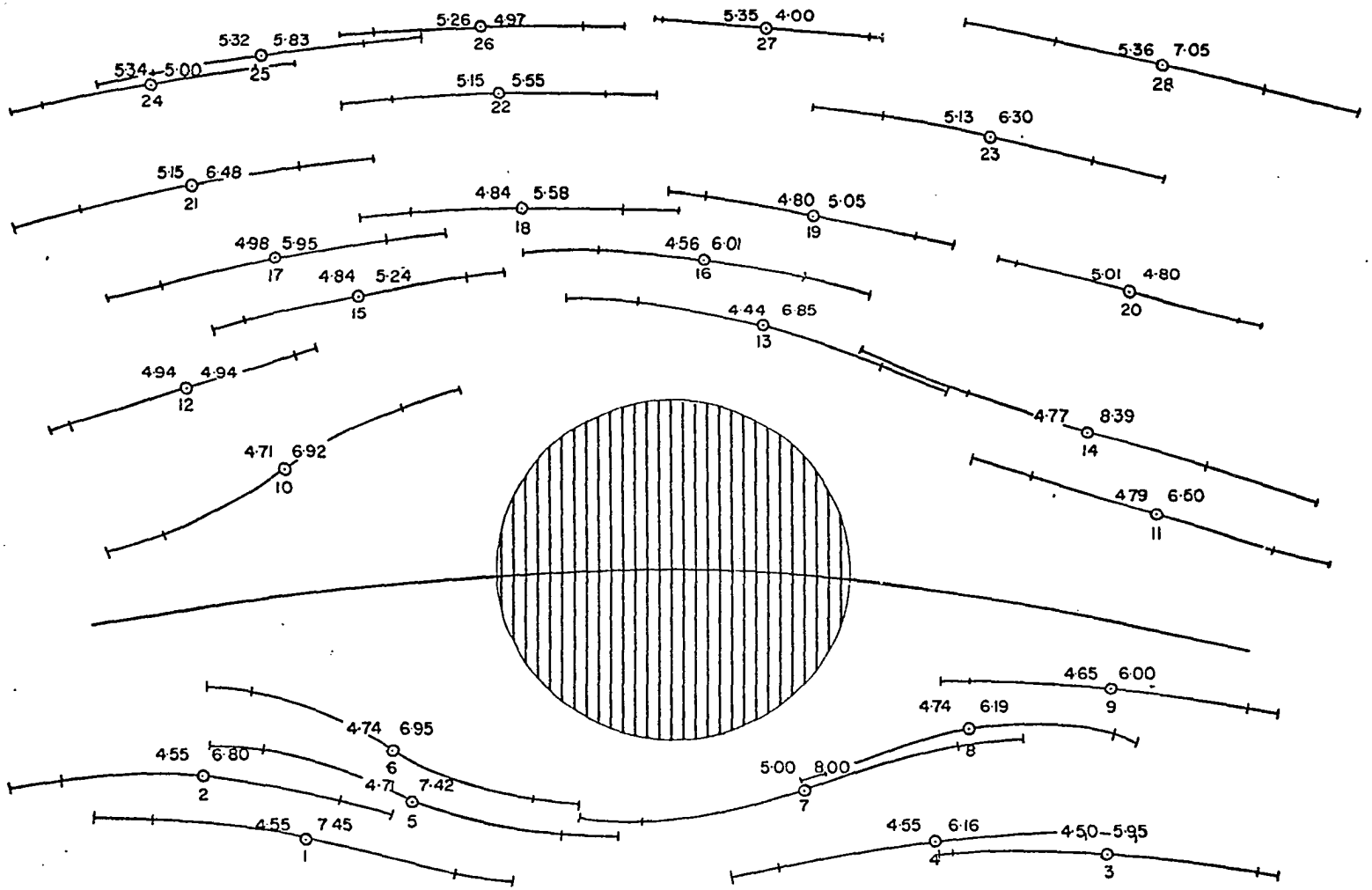

Figure 4.8. Theoretical and experimental streak lengths for photograph 16. Measured values plotted on right of point and theoretical values on left. Each point labeled below for identification.

V - CONCLUSIONS AND SUGGESTIONS FOR FUTURE WORK

At the initial development the storm cloud is influenced by the converged air and by the ambient flow that it obstructs. The balance of these two effects controls storm motion while enhancing its development to a severe storm by contributing toward increasing the convergence. Atmospheric drag makes the cloud curve in the direction of vertical wind shear and veer, and causes circulation to be induced about the cloud. This may contribute to transverse forces which cause the storm to increase its motion toward the inflowing low level air and, thereby, contribute toward increasing the convergence. Where circulation is induced and significant transverse forces are operating, the storm contains the necessary ingredients to support its severity.

The circulation that could be induced by a storm cloud growing in a veering and shearing environment, whose path is curved in response to the drag effects of the ambient air, is significant since it is equivalent to tornado circulation. If there were some mechanism to concentrate the vorticity at the cloud edge into the area of a tornado vortex (diameter about 1 km) while conserving angular momentum, then presumably, tornadic velocities could be achieved by sufficient curving of the cloud along its path.

Combining the low level momentum effect with the middle level drag effect, the first two terms in the mathematical formulation for storm motion, has resulted in some restrictions in the total number of combinations of lower and middle layer air velocities that can exist for constant storm motion. In the future, considering the circulation, the third term, in combination with the first two, should restrict the number of combinations further and ultimately lead to accurate prediction of storm motion. The additional terms, such as the pressure differential term and the residual propagation term should be investigated as measurements become more plentiful.

The basic hydrodynamic experiment has been performed and, although it has not verified the quantitative relation that will allow a detailed computation of circulation, we can now be more assured than before that the experimental analogy to the atmosphere exists. This means that perfecting experimental apparatus and technique should be emphasized and more experiments should be undertaken.

Hydrodynamic experiments of curving cylinder motion made in a fluid that is veering and shearing with height, would be more closely related to a severe storm environment. These experiments should be made also using cylinders whose roughness varies with depth in the veering and shearing fluid. It is hoped these experiments will provide both renewed impetus and encouragement to seek information in existing data in addition to providing guides for future case studies investigating the induced

response of the fluid to the curved motion of the cylinder.

In the past, hydraulic analogies to explain measured phenomena have been used successfully, especially in the case of pressure jumps. The increasing number of measurements of storm motions that differ in direction on both sides of the direction of the mean wind throughout the storm depth has led some investigators to posit hydrodynamic analogies with barrier flow.

Goldman (1962) recognized the similarity between the motion of storm radar echoes and the hydrodynamic source plus pure translation. He explained the effect of circulation (1966) and later (1967, 1968) developed a model of three dimensional airflow in a severe storm, based on the analogy to barrier flow. Sasaki and Syono (1966) used a doublet to represent the low levels of a moving hurricane. The same analogy was used by Charba and Sasaki (1968) to explain the anomalous motion of severe storms on a particular day. This same case was studied by Fujita and Grandoso (1968) with a resulting model development, based on Karman vortex theory. Although their development did not distinguish between free (Karman) vortices and bound vortices (in storms with substantial updrafts and circulation about them), their approach is in the direction of hydrodynamic analogies. More recently, Darkow (1969) suggested considering horizontal shear to account for transverse forces on a severe storm. Barnes (1969) used barrier flow concepts accompanying his description of a radiosonde ascent within an updraft. In his description of the sequence of events he

included the anticyclonic curving of radar echo paths during their early stage of development in the veering environment.

With the seeds of hydrodynamic barrier flow theory being planted somewhat more firmly in the minds of empiricists, perhaps more studies will include investigation of the early stage of storm development to check the effect of a veering environment on the storm's path against the eventual development of circulation about the storm.

BIBLIOGRAPHY

Achtmeyer, Gary L. "On the Correlation Between Severe Weather and the Trajectories of Deviate Storms Over the Midwest on August 25, 1965." Rept. No. 69-5. Florida State University, 1969.

_____. "Some Observations of Splitting Thunderstorms Over Iowa on August 25-26, 1965." Proceedings of the Sixth Conference on Severe Local Storms, American Meteorological Society, Chicago, Illinois, April 1969.

Barnes, S. L. "On the Source of Thunderstorm Rotation." NSSL Tech Memo 38, ESSA, U. S. Dept. of Commerce, 1968.

_____. "Some Aspects of a Severe, Right-moving Thunderstorm Deduced from Mesonetwork Rawinsonde Observation." Proceedings of the National Severe Storms Conference, Chicago, 1969.

Bonner, W. "An experiment in the Determination of Geostrophic and Isallobaric Winds from NSSP Pressure Data." Mesomet. Proj. Research Paper No.26, Dept. of the Geophysical Sciences, The University of Chicago, 1963.

Browning, K. A. and T. Fujita. "A Family Outbreak of Severe Local Storms-A Comprehensive Study of the Storms in Oklahoma on 26 May 1963." Part I. Special Report #32, Air Force Cambridge Res. Lab., 1965.

_____. "Airflow and Precipitation Trajectories within Severe Local Storms Which Travel to the Right of the Winds." J. Atmospheric Science 21, 6, 634-639, 1964.

_____. and F. H. Ludlam. "Airflow in Convective Storms." Quar. J. Royal Meteorology Socity 88, 117-135, 1962.

Charba, J. and Y. Sasaki. "Structure and Movement of the Severe Thunderstorms of 3 April 1964, as Revealed from Radar and Surface Mesonetwork Data Analysis." Tech Memo. ER LTM-NSSL 41, ESSA Res. Lab. 1968.

Darkow, G. L. "Deflecting Forces on Non-rotating Convective Systems to Environmental Shear." Sixth Conference on Severe Local Storms, Chicago, 1969.

Fankhouser, J. C. "Thunderstorm-Environment Interaction Revealed by Trajectories in the Mid-Troposphere." NSSL Tech. Memo, ESSA U. S. Dept. of Commerce, 1968.

Foster, D. S. and F. C. Bates. "A Hail Forecasting Technique." Bull. Am. Meter. Soc. 37, 135-141, 1956.

Fujita, T. "Analytical Mesometeorology: A Review." Meteor. Mono. 5, No. 27, 77-123, 1963.

_____. and H. Grandoso. "Split of a Thunderstorm into Anticyclonic and Cyclonic Storms and their Motion as Determined from Numerical Model Experiments." SMRP No. 62, Dept. of the Geophysical Sciences, The University of Chicago, 1966.

Goldman, J. L. "The High Speed Updraft - the Key to the Severe Thunderstorm." J. Atmospheric Science, 25, 2, 222-248, 1968.

_____. "Study of the Development of Prefrontal Squall Systems Using NSSP Network Data." Research Paper No. 10. Mesomet. Proj. Dept. of the Geophysical Sciences, The University of Chicago, 1962.

_____. "The Role of the Kutta-Joukowski Force in Cloud Systems with Circulation." NSSL Tech Rept. 27, U. S. Weather Bureau, Washington, D. C., 1966.

_____. "A Parameterized Model of Air Flow and Rain Distribution in a Steady State Severe Storm." Final Rept. NSSL Contract E36-67(N) ESSA,U. S. Dept. of Commerce, 1967.

Hoerner, S. F. Fluid-Dynamic Drag. S. F. Hoerner, Midland Park, N. J., 1958.

Kuo, H. L. "On the Dynamics of Convective Atmospheric Vortices." J. Atmospheric Science, 23, 25-42, 1966.

Miller, R. C. Notes on Analysis and Severe-Storm Forecasting Procedures of the Military Weather Warning Center. Air Weather Service, (MAC) U. S. Air Force, 1967.

Newton, C. W. and J. C. Fankhauser. "Movement and Development Patterns of Convective Storms and Forecasting the Probability of Storm Passage at a Given Location." NSSP Rept. 22. Washington, D. C., U. S. Weather Bureau, 1964.

Sasaki, Y. and S. Syono. "Motion of the Vortex with Pressure and Inflow Which are not Circular Symmetry." Ref. ARL-1470-3, Atmos. Res. Lab. Norman, Okla: University of Oklahoma Research Institute, 1966.

LIST OF SYMBOLS

Symbol	Definition
A	area of cylinder
$\vec{A}_s$	storm acceleration
$\vec{C}$	storm velocity
C_D	drag coefficient
$\frac{d\vec{C}}{dt}$	time rate of change of the storm's motion, acceleration
D	diameter of upward motion, diameter of cylinder representing storm volume
F	force
h	height of cylinder representing storm volume
J_i	inward flux of air below the inversion converged into the storm
J_u	upward flux of air inside storm
K	curvature
ℓ	width of inflowing channel of air
m	mass of storm
M	middle level moisture
P	difference in ambient velocities
$\vec{\nabla}P$ diff.	gradient of differential pressure

Symbol	Definition
Q	convection contributing quantity
r	radius
r_c	radius of cylinder
r_s	distance from center of the cylinder to streak's midpoint
R	radius of swivel arm
R_{PR}	residual acceleration
R_s	distance from swivel to streak's midpoint
s	stability index
S_r	theoretical streak length at any distance r
S_Ω	contribution to streak length due to motion of cylinder about the swivel
$\mathscr{g}$	mass of air taken into storm per unit time
S_ω	contribution to streak length due to circulation about the cylinder
t_e	exposure time
U	velocity of ambient air relative to moving storm
V	velocity of ambient air relative to ground
V_θ	tangential velocity about the cylinder
$V_{\theta s}$	tangential velocity about swivel
$\vec{V}$	velocity vector

Symbol	Definition
w	the velocity representative of the mean mass weighted vertical flux
z	depth of inflowing air, to height of inversion
α	angle subtended at cylinder by rotation
ζ	vorticity
θ	angle subtended by cylinder revolving at swivel
ρ	mean density of air
Ω	angular velocity at swivel
ω	angular velocity
ϑ	angle described by the two radii r_s and R_s
Γ	circulation about the storm

SUBSCRIPTS

Symbol	Definition
c	at cylinder
D	middle (dry level)
e	exposure
M	middle layer
P	upper (plume level)
PR	propagation
s	at swivel, or streak
S_1	inner arc length
S_2	outer arc length
sia	sub-inversion layer
W	low (wet level)
Δs	$S_2 - S_1$
θ	in the direction theta
Ω	contribution due to Ω
ω	contribution due to ω
θs	tangential velocity about the swivel